UCRL--21213

DE90 012893

IN SITU DETECTION OF ORGANIC MOLECULES: OPTRODES FOR TCE AND $CHCl_3$

S. Michael Angel, Kevin C. Langry,
and
Maureen N. Ridley

May 1990

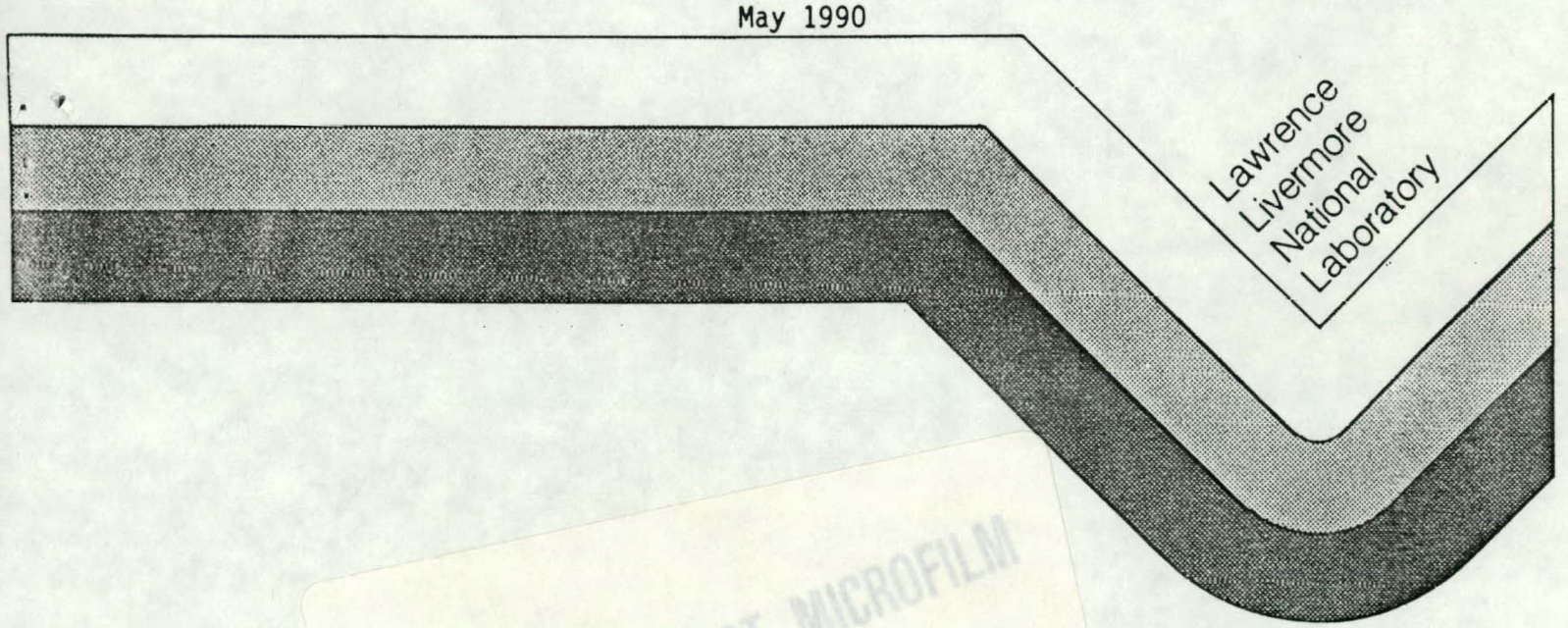

DISCLAIMER

PHASE II FINAL REPORT.
IN SITU DETECTION OF ORGANIC MOLECULES:
Optrodes for Trichloroethylene and Chloroform.

S. Michael Angel
Kevin C. Langry
Maureen N. Ridley

September 12, 1989

Prepared by

ENVIRONMENTAL SCIENCES DIVISION
LAWRENCE LIVERMORE NATIONAL LABORATORY
P.O. Box 5507
Livermore, California 94550

Sponsored by the

U.S. DOE HAZARDOUS WASTE REMEDIAL ACTIONS PROGRAM
Support Contractor Office
Oak Ridge, Tennessee 37831
operated by
MARTIN MARIETTA ENERGY SYSTEMS, INC.
for the
U.S. DEPARTMENT OF ENERGY
under Contract DE-AC05-84OR21400

TABLE OF CONTENTS

ABSTRACT

We have developed new absorption-based chemical indicators for detecting chloroform ($CHCl_3$) and trichloroethylene (TCE). These indicators were used to make very sensitive optical chemical sensors (optrodes) for each of these two contaminants. Concentrations below 10 ppb can be accurately measured using these sensors. Furthermore, they are selective and do not respond to similar contaminants commonly found with TCE and $CHCl_3$ in contaminated groundwater. In addition, the sensor response is linearly proportional to the chemical concentration. In this report, we describe the details of this optrode and the putative reaction sequences of the indicator chemistries with $CHCl_3$ and TCE and present an analysis of the spectral data obtained from the reaction products.

A key part of the development of this optrode was designing a simple readout device. The readout is a dual-channel fiber-optic fluorimeter modified to measure transmission or absorption of light. The system is controlled by a lap-top microcomputer and is fully field portable.

In addition to describing the final absorption optrode, details of the chemical indicator reactions are presented for both absorption- (colorimetric) and fluorescence-based optrodes. Insights gained in these chemical investigations will be useful in developing future optrodes.

Finally, we report on the syntheses of several compounds used to evaluate the indicator chemical reactions that led to the development of the absorption optrode. Much of this information is presented as an Appendix to this report.

OBJECTIVES

The long-term objective of this research is to develop a fiber-optic-based system for monitoring contaminant species in groundwater. These efforts require the development of optical chemical sensors (optrodes) that are compatible with optical fiber spectrometers. Spectrometers designed specifically for fiber-optic chemical sensors were previously developed in our laboratory, as were optrodes for selected chemical species. The main objective of the research phase of this project is to develop a chemical indicator for an optrode configuration that will allow selective detection and quantification of trichloroethylene (TCE). This task has been successfully completed.

The first task of the optrode development program was to elaborate the reaction mechanism of an existing chemistry used for nonspecific detection of organohalides. This chemistry was adapted from a clinical assay used to determine organochloride contamination, and we found that this method is not directly suited for incorporation into fiber-optic sensors. However, by understanding the details of the clinical assay and the reaction chemistry of organohalides, specific approaches can be suggested to provide selective, sensitive, and stable detection systems for the organohalide optrodes. This task has been completed.

A second task of this project was to develop indicator chemistries that could be used in combination with optical fibers to monitor TCE selectively in the presence of chloroform. This task has also been successfully completed. A TCE-selective optrode has been completed that can measure less than 10 ppb TCE in water. This particular optrode is moving into the Demonstration Phase.

In FY 1990 another research task will be added to this project. We will attempt to build on our understanding of chlorinated hydrocarbon chemistry and optrodes and attempt to develop new optrodes for carbon tetrachloride (CCl_4) and perchloroethylene (C_2Cl_4). Other contaminants will be selected as appropriate.

LIST OF FIGURES

LIST OF TABLES

LIST OF ACRONYMS AND DEFINITIONS

AMP: 2-(aminomethyl)pyridine

BAH: benzyltrimethylammonium hydroxide

$CHCl_3$: chloroform

DCA: dichloroacetylene

DOE: Department of Energy

EIMS: electron impact mass spectrometry

GC: gas chromatography

HRMS: high resolution mass spectrometry

HAZWRAP: Hazardous Waste Remedial Actions Program

IR: infrared

LLNL: Lawrence Livermore National Laboratory

mp: melting point

ms: mass spectrometry

NMR: nuclear magnetic resonance

OHER: Office of Health and Environmental Research

optrode: fiber-optic-based chemical sensor

TBAH: tetrabutylammonium hydroxide

TCE: trichloroethylene

TEGD: tetraethyleneglycol dimethyl ether

TLC: thin layer chromatography

uv: ultraviolet

Vis: visible

ACKNOWLEDGMENTS

The authors wish to thank Dr. James Epler of the U.S. Department of Energy (DOE) Hazardous Waste Remedial Actions Program (HAZWRAP) of Martin Marietta Energy Systems, Inc., for his gracious assistance and encouragement.

This project is funded by the U.S. DOE Hazardous Waste Remedial Actions Program at Martin Marietta Energy Systems, Inc., under contract DE-AC05-84OR21400. This report covers work funded by HAZWRAP performed between July 16, 1988 and August 25, 1989.

Work was performed under the auspices of the U.S. DOE by Lawrence Livermore National Laboratory under Contract W-7405-ENG-48.

1. INTRODUCTION

Chlorinated hydrocarbons have been used extensively over the last 40 years in a variety of commercial and defense-related industrial processes. The excellent solvent properties of these chemically inert compounds have made them the primary industrial degreaser employed in processes ranging from dry cleaning clothing to degreasing aircraft engines. Moreover, these compounds represent an important class of solvents used in many chemical processes. However, it is now recognized that many, if not all, of these chlorinated hydrocarbons pose a serious health risk to individuals exposed to them. Although current laboratory and manufacturing practices are strictly regulated to ensure the proper management of these compounds, earlier disposal methods for waste chemicals and solvents were not designed with consideration of the long-term stability of these reagents. Consequently, many chlorinated hydrocarbons have found their way into the consumable groundwater supply where they represent current and potential hazards to public health.

Fiber-optic chemical sensors (optrodes) are becoming increasingly popular because of their potential to measure samples remotely and *in situ*. Their use has become sufficiently widespread that several literature reviews have recently appeared.[1-3] Fiber-optic sensors are small, are immune to electrical and radio frequency noise, and permit measurements to be made using remotely located instrumentation that minimally disturbs the sampling region. Optrodes are basically of two types: those that rely on a change in the physical characteristics of the optical fiber itself, and those that use the optical fiber simply as a light pipe to connect a spectrometer to a remotely located optical sensor.

Several areas of fiber-optic sensor research are being pursued by the Environmental Sciences Division at Lawrence Livermore National Laboratory (LLNL). These include the development of new, chemically specific, optrodes[4,5] [Hazardous Waste Remedial Actions Program (HAZWRAP) funded] and the development of new, remote spectroscopic techniques[6] [Office of Health and Environmental Research (OHER) funded]. Also, we are investigating some applications of these devices both inside and outside the laboratory. New laboratory applications that are being investigated include monitoring anaerobic microbial degradation (OHER) and measuring transport properties of groundwater contaminants in porous soil systems (OHER).[7] Recently demonstrated field applications include measuring organochlorides in contaminated aquifers,[8] measuring chlorophyll fluorescence from marine algae *in situ* using a ship-towed fiber-optic probe,[9] and measuring temperature profiles in a geothermal well.[10]

At LLNL, we are developing optrodes to detect and monitor environmental pollutants for HAZWRAP. The long-term objective of this research project is to develop an entire fiber-optic-based system for monitoring environmental contaminants, and the approach we are pursuing emphasizes two primary objectives. The first goal is to understand the chemistry of the contaminant, so that the most effective detection scheme can be developed. The second goal is to design optrodes that best exploit the photophysical properties of the detection scheme. This philosophy, applied to both instrument design and optrode development, removes the restriction that the optrodes be strictly based on a specific optical property, such as fluorescence, and encourages the development of a broad array of sensors with optimal detection efficiencies.

In previous reports we reviewed the chemistry of trichloroethylene (TCE) and chloroform ($CHCl_3$) and described a new chemical detection scheme that produces fluorescent products from these two pollutants. We incorporated this new chemistry into a fluorescence-based optrode and provided preliminary data showing the optrode response to low parts-per-million levels of TCE-contaminated water. In this report, we describe in more detail the chemistry of these fluorescence-based optrodes.

More importantly, we also report on a new optrode design that exploits the light absorption properties of a TCE and $CHCl_3$ indicator chemistry that affords detection of these groundwater contaminants at the low parts-per-billion level.

2. RESULTS IN FISCAL YEAR 1989

2.1 TRICHLOROETHYLENE AND CHLOROFORM OPTRODE EVALUATION

This research project has led to the development of a very sensitive fiber-optic chemical sensor (optrode) for trace-level measurements of trichloroethylene (TCE) and chloroform ($CHCl_3$). Before the final design was completed, we investigated the chemistry of these chlorinated hydrocarbons and tested several optrode-design concepts, including fluorescence-based and colorimetric(absorption)-based versions. The absorption optrode was by far the most successful in terms of optrode sensitivity, reproducibility, and simplicity. The performance of the absorption optrode will be described in the remainder of this section. Later sections will describe in more detail the indicator chemistry that is the basis of the optrode measurement. Also, later sections will describe the fluorescence chemistries that were studied and their disadvantages for these particular contaminants. It should be noted that the development of the fluorescence chemistries will probably be useful in developing future chlorinated hydrocarbon optrodes.

The dual-wavelength absorption optrode is a new type and did not appear in the literature at the time it was developed for HAZWRAP. Recently, we described this device at several meetings and wrote three papers on this topic. This optrode was developed specifically to measure TCE and $CHCl_3$ in groundwater and in unsaturated contaminated soils (vadose zone). This device shows dramatically improved performance over previously reported fluorescence-based sensors.[8] The new optrode measurement is based on the absorption of light by a colorimetric indicator held in a small-diameter capillary tube as shown in Figure 1. Two 320-μm-core optical fibers are sealed in a 2-mm-diam glass capillary tube that holds about 20 μL of the optrode reagent. The open end of the capillary tube is sealed with a white Teflon membrane. The analyte vapor diffuses rapidly through the Teflon membrane and reacts with the optrode reagent, producing a highly colored product that absorbs light at 530 nm. One optical fiber delivers a very-low-intensity probe light to the optrode. The light passes through the reagent and is attenuated at 530 nm by the colored product that develops. The light then reflects from the Teflon membrane and passes through the reagent a second time, providing further attenuation (and higher sensitivity). The attenuated light is then collected by the second optical fiber and is delivered to a filter fluorimeter for analysis.

An internal intensity reference is provided by measuring light at a wavelength that is transmitted through the optrode without attenuation (610 nm). This internal reference is crucial to the success of the optrode. It provides compensation for light intensity variations that result from

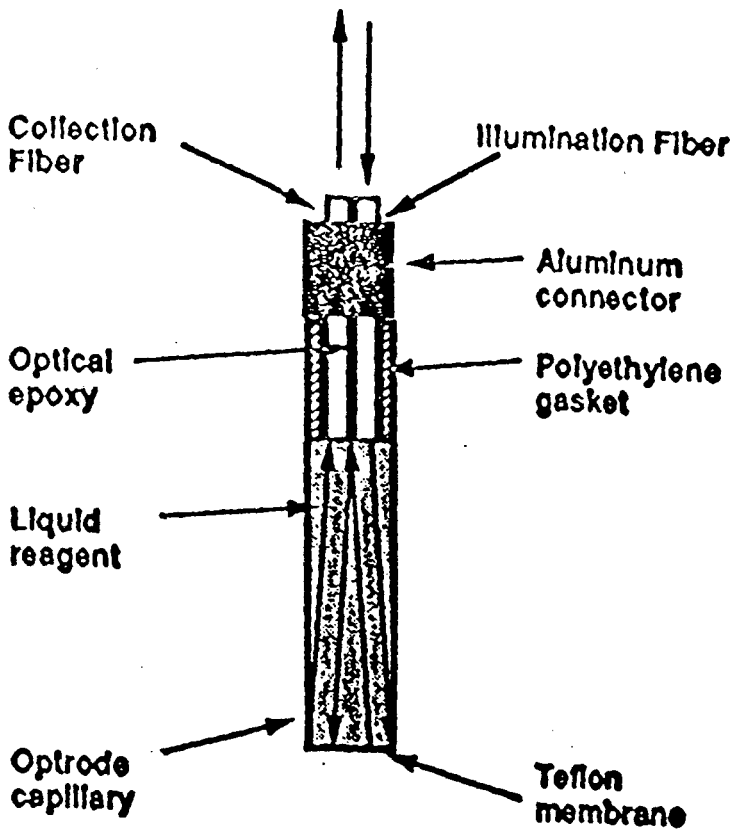

Figure 1. Schematic of the dual-wavelength absorption optrode.

the source, bending in the fiber, amount of reagent, and changes in the Teflon membrane. The ratio of the two signals [transmission (T)] is proportional to the analyte concentration and is independent of the light intensity. The absorbance (A),-log(T), is linearly proportional to the analyte concentration.

The optrode reagents are different for TCE and $CHCl_3$. For $CHCl_3$, the reagent is a mixture of 87.5% pyridine (by volume) and 12.5% tetrabutylammonium hydroxide (TBAH) (40% aqueous solution). For TCE, the reagent is 99% by volume of pyridine and 1% TBAH solution. We have also experimented with adding long-chain ethers to the TCE reagent to improve the solubility of the TCE. We found that the addition of 40% tetraethyleneglycol dimethyl ether (TEGD) to 60% of the $CHCl_3$ reagent gives very good response to TCE. In the presence of strong base (TBAH), both analytes form transient species that react with the pyridine to form colored products. The amount of color that develops is proportional to the vapor-phase concentration of the analyte. Both reagents are very stable and can be used for several weeks without loss of response. The development of the indicator reagents is described in detail in a later section.

The fiber-optic spectrometer used for this work is shown in Figure 2. The illumination block consists of a 5-W quartz-halogen lamp whose output is chopped at 30 Hz and imaged onto the excitation optical fiber. The ultraviolet (uv) wavelengths are removed from the excitation light with a long-wavelength pass filter. This is done to minimize the potential for photodegradation in the optrode. The light that returns from the optrode is analyzed at 530 and 610 nm using a fiber-optic fluorimeter (Douglas Instruments Model II Fiber-Optic Fluorimeter) modified for dual-wavelength detection. A dichroic beam splitter separates the incoming optrode signal into a red-wavelength component (wavelengths longer than 550 nm are transmitted) and into a green-wavelength component (wavelengths shorter than 550 nm are reflected). The reflected component is then passed through a 530-nm band pass filter (~30-nm band width) and is detected by a silicon photodiode. The component transmitted through the dichroic beam splitter is passed through a 610-nm band pass filter (~25-nm band width) and is detected by a second silicon photodiode. The optrode response is taken as the ratio of the 530- and 610-nm signals. The normalized ratio is equivalent to transmission. The decrease of T is monitored as a function of time.

In the laboratory experiments, measurements were made using 10- and 160-ft-long optical-fiber cables. The length of the fiber seemed to have no effect on the normalized response of the optrode. Measurements were made in 250-mL flasks fitted with a Teflon valve that sealed around the stainless-steel optrode housing. About 125 mL of analyte was used in the 250-mL flask. The optrode was held

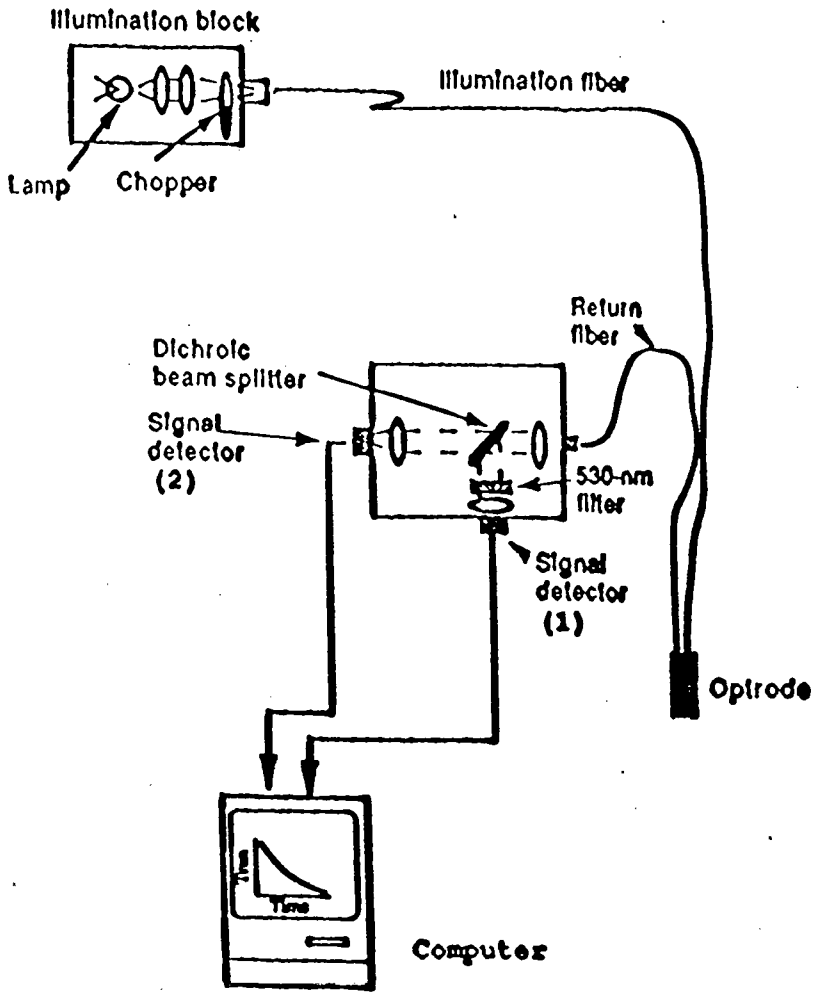

Figure 2. Principal components of the dual-channel fiber-optic fluorimeter used to measure the dual-wavelength absorption optrode.

about 2 in. above the analyte solution by the Teflon stopper that sealed the flask during the measurement. The contents of the stoppered flask were stirred 5 to 10 min before and during the optrode measurement. Changes in the stir rate and changes in the height of the optrode above the solution did not significantly affect the optrode response.

Figure 3 shows the decrease in transmittance (T) of the $CHCl_3$ optrode plotted versus time of exposure time to aqueous concentrations of $CHCl_3$ that range from 10 to 500 ppb. (All concentrations referred to in the text are the original aqueous-phase concentrations.) The response at 10 ppb is much greater than the noise level, indicating that lower $CHCl_3$ concentrations can be measured. The vapor-phase $CHCl_3$ concentrations for these solutions were about 10% of the original solution concentrations. The amount of $CHCl_3$ in the vapor phase was independently measured using ^{14}C-labeled $CHCl_3$, and also by gas chromatography (GC). The vapor-phase concentrations differed slightly from the expected Henry's law equilibrium values.

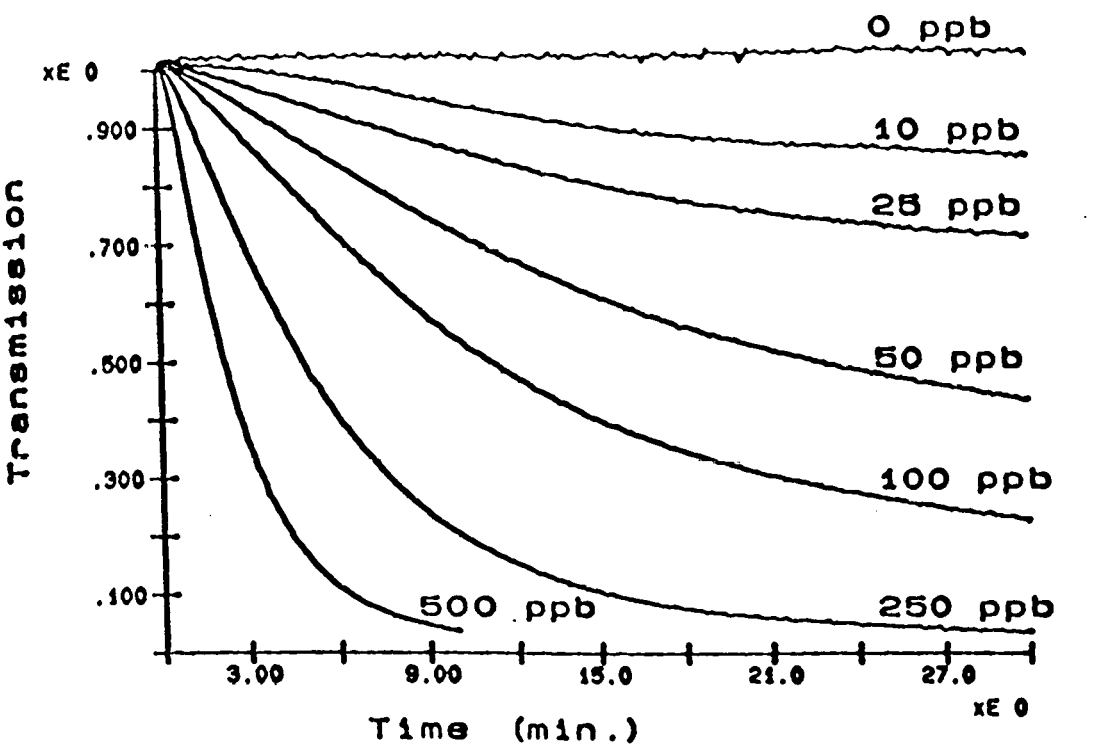

Figure 3. Normalized transmission response versus time of the chloroform ($CHCl_3$) optrode to different aqueous-phase concentrations of $CHCl_3$.

A plot of -log(T) versus $CHCl_3$ concentration produces a linear calibration curve (see Figure 4) for concentrations below 1 ppm and using a 15-min exposure time. At higher concentrations, the response is not linear using such a long exposure time because the reference wavelength is attenuated by the intensely colored product that develops in the optrode. However, a linear working curve would result for higher concentrations by using a much shorter exposure time. Attenuation of the reference wavelength leads to artificially high values of T and low values of -log(T).

The accuracy of the $CHCl_3$ optrode was determined by making five separate measurements of a 500-ppb $CHCl_3$ solution using five different optrodes (Figure 5). The sample standard deviation of the optrode responses was taken after 15 min. The average response after 15 min was 89.8 ±6.2%.

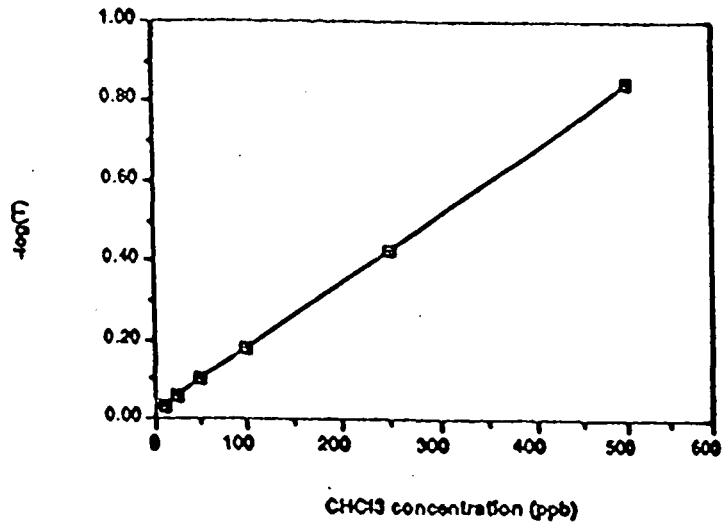

Figure 4. Response of the chloroform ($CHCl_3$) optrode after 15-min exposure to different aqueous-phase $CHCl_3$ concentrations.

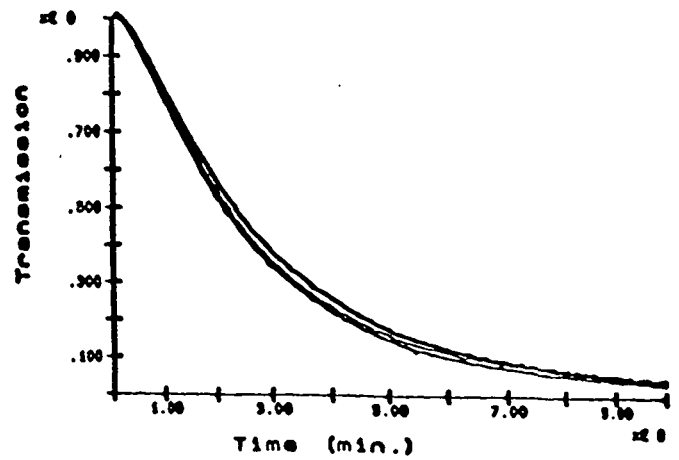

Figure 5. Variability between measurements using different chloroform ($CHCl_3$) optrodes and 500-ppb $CHCl_3$ samples.

Figure 6 shows the decrease in transmittance (T) of the TCE optrode plotted versus time of exposure time to aqueous concentrations of TCE that range from 10 to 500 ppb. As shown above for the $CHCl_3$ optrode measurements, the response to the 10-ppb TCE solution is well above the noise level. The vapor-phase concentrations of TCE were 12 to 14% of the original solution concentrations. This was confirmed by ^{14}C-labeling and also by GC analysis of vapor samples. The accuracy of the TCE optrode was determined as indicated above using a 500-ppb TCE solution, except that measurements were taken after 30 min. The average response after 30 min was 62.4 ±8.3%.

A plot of -log(T) versus TCE concentration is shown in Figure 7. It is also linear and reproducible as indicated above for the $CHCl_3$ optrode. The most linear calibration curves are obtained by using the lowest possible lamp power. However, even at low lamp powers, the calibration is still nonlinear above 1 ppm because of attenuation at the reference wavelength by the intensely colored product that develops in the optrode. As indicated above, a shorter exposure time would be used for higher concentrations.

The data presented above indicate that this optrode is ready for demonstration. The sensitivity and accuracy are competitive with field GC measurements, as is the speed of the measurement.

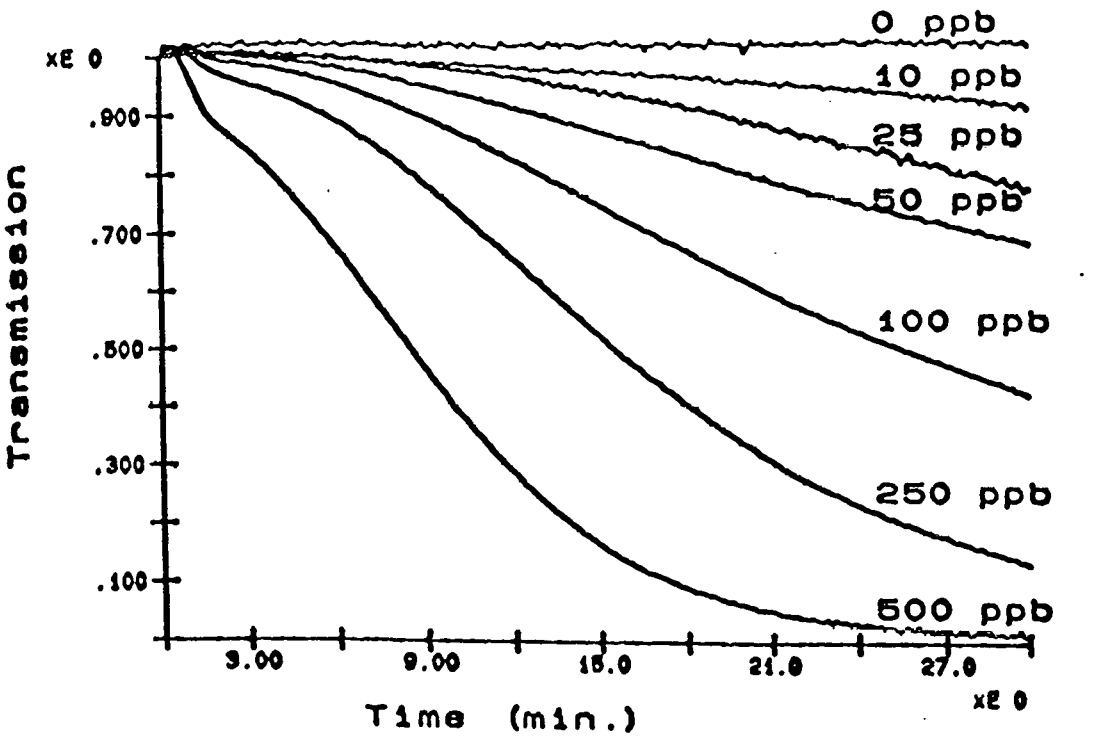

Figure 6. Normalized transmission response versus time of the trichloroethylene (TCE) optrode to different aqueous-phase TCE concentrations.

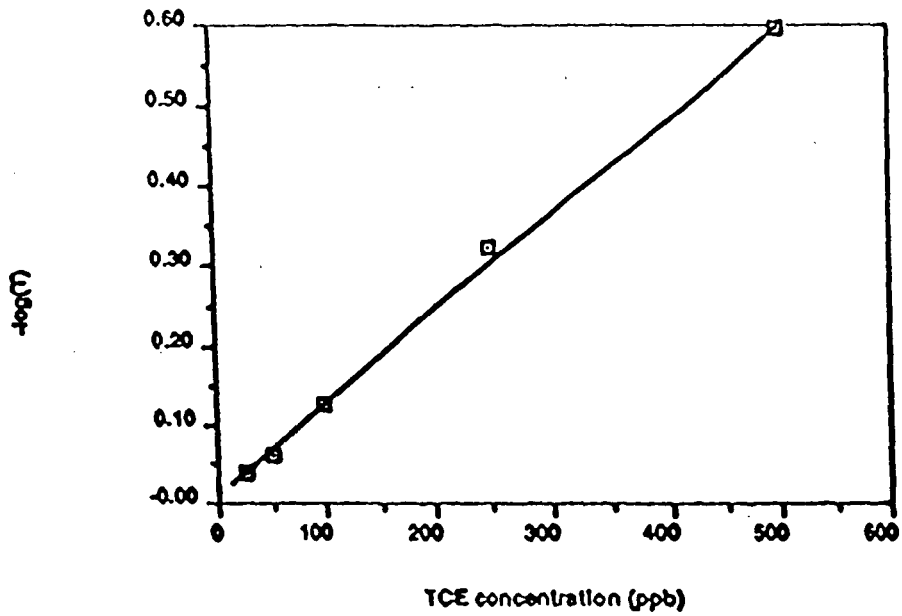

Figure 7. Response of the trichloroethylene (TCE) optrode to different aqueous-phase TCE concentrations using 15-min exposures.

2.2 CHEMISTRY OF THE NEW ABSORPTION-BASED OPTRODES

The indicator chemistry of the absorption optrode is based on the ring-opening reaction that pyridine experiences when it is N-alkylated in the presence of hydroxide ions. We reviewed this chemistry in an earlier report,[11] but here we present some new spectroscopic results that can be used to make the probe more sensitive and selective than previously discussed.

The absorption optrode indicator chemistry is modeled after the color-forming reaction that occurs between pyridine and $CHCl_3$.[12] In this reaction, pyridine reacts with $CHCl_3$ in the presence of strong base to form the formamidine **1** and imine **2**. Hydrolysis of these compounds gives rise to the

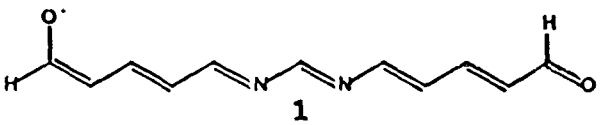

1

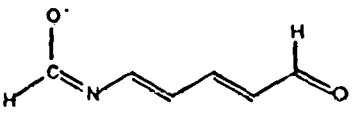

2

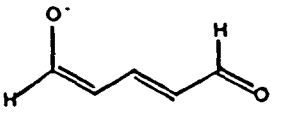

3

dialdehyde **3**. Under the same conditions, TCE also forms colored products,[13] and it is likely that this reaction follows a sequence similar to the $CHCl_3$ reaction. Dichloroacetylene (DCA) derived from TCE probably reacts with pyridine to generate an N-alkylated pyridinium species. A similar reaction is known to occur between DCA and imidazole to form the corresponding N-(2-chloroethenyl)imidazole.[14] We noted in another report that DCA might react with pyridine to form the bicyclic compound **4** in the same way that dimethyl acetylenedicarboxylate reacts with pyridine to form **5**.[15] However, the very low concentrations of TCE and DCA that

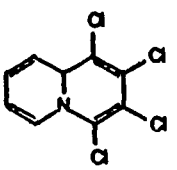

4

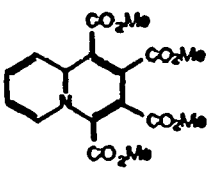

5

exist at any time in the optrode (see Table 1, pg. 23) indicates that a more likely reaction is one in which the alkylated pyridinium intermediate undergoes ring opening to form an imine. This scenario is more consistent with the established chemistry of pyridine, the relative concentrations of optrode reactants, and visible (VIS) spectral data of the reaction between TCE and pyridine in the presence of base.

We followed the reaction of TCE with pyridine and TBAH by monitoring the VIS absorption spectrum of the reaction solution. In an effort to mimic the way an optrode functions, the solution of pyridine containing 2% TBAH was exposed to TCE vapor while the cuvette remained in the spectrometer. Almost immediately upon exposure, the solution at the top of the cuvette developed a light yellow color. The solution appeared to remain homogeneous as the pigment migrated unevenly to the bottom of the cuvette. An absorbance spectrum of the solution shows three absorbance maxima of nearly equal intensity at 360, 380, and 420 nm. However, the intensity of these maxima is questionable because the spectrum was obtained as the color migrated to the bottom of the cuvette in concentrated streams. Within minutes the solution became too optically dense to follow spectrally, so the TCE vapor was removed and the reaction mixture diluted with the pyridine-TBAH solution. The diluted solution exhibits an absorbance spectrum with only one peak maximum in the visible region at 413 nm (Figure 8). The intensity of this peak diminishes with time, as a new peak develops at 360 nm (Figure 9). The presence of an isosbestic point at 380 nm indicates that the compound possessing the 413-nm band is converted directly into the compound that exhibits the 360-nm absorbance. The direct addition of a dilute solution of TCE to the pyridine-TBAH mixture also results in the immediate formation of a single absorbance band at 413 nm that gives way to the 360-nm absorbance. We have not yet isolated the compounds responsible for these absorptions, but, based on the similarity of this reaction to the chemistry of the Fujiwara reaction, the 360-nm band probably belongs to glutaconaldehyde **3** and the 413-nm absorbance may result from a compound similar to imine **6**.

6 **7**

The results we obtained in the cuvette experiments appear different from those seen for the same reagents in the optrode. When an optrode charged with pyridine containing 1% TBAH solution is exposed to head-space vapor from water contaminated with parts-per-billion levels of TCE, an intense purple color develops in the indicator reagent. In contrast to these results, none of the solutions prepared by the direct addition of substantially greater concentrations of TCE developed a similar absorbance. However, the purple color was observed in solutions consisting of pyridine (90%), TBAH (1%), and water (9%). The presence of this additional water is critical to the formation of the intense purple color. Apparently the reagent in the optrode manages to absorb enough water from the atmosphere to permit development of the purple pigment.

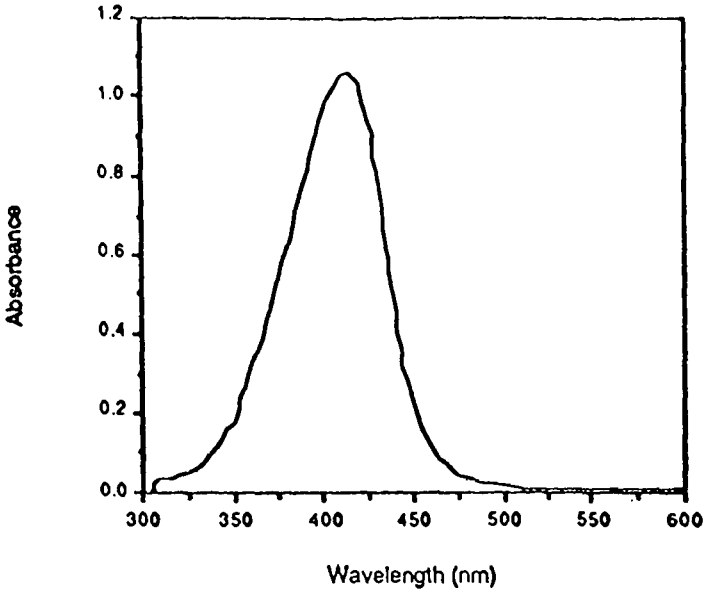

Figure 8. Absorption spectrum resulting from the reaction of trichloroethylene (TCE) vapor with a solution of pyridine (98%) and tetrabutylammonium hydroxide (TBAH) (2%).

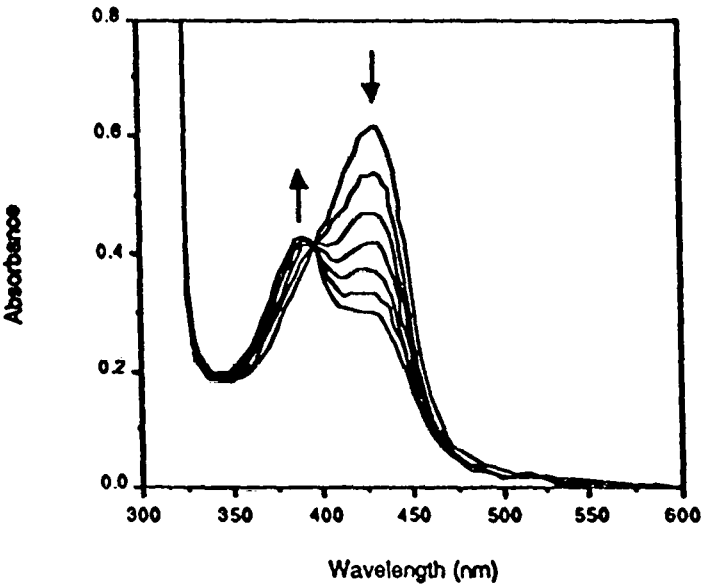

Figure 9. Degradation of the 413-nm band formed from the reaction of trichloroethylene (TCE) vapor with a solution of pyridine (98%) and tetrabutylammonium hydroxide (TBAH) (2%).

Water clearly had a dramatic effect on the development of color in the indicator reagent, so we examined the reaction in more detail, with specific attention directed at the potential for developing a reagent that is more sensitive and more specific to TCE. The addition of 0.5 µL of neat TCE to a 3-mL solution of the optrode reagent, consisting of 90% pyridine, 1% TBAH, and 9% water, causes the reaction mixture to turn deep purple with the appearance of a single absorption band centered at 550 nm (Figure 10). The broad 550-nm band requires several minutes to develop to its maximum intensity and is reasonably stable in the basic reaction medium. Once the peak reached a maximum intensity, the decay of the 550-nm absorbance was monitored with sequential scans over a period of 100 min. The resulting spectra are shown in Figure 11. The decay of the 550-nm band is concurrent with the appearance of a new band at 470-nm and an increase in the absorbance near 360 nm. Because the intensity of the isosbestic point at 480 nm is independent of the rate of decomposition of the purple reaction product, this wavelength may be a valuable region on which to base the measurement of TCE concentrations with future optrodes.

If water is not added to the solution of pyridine (99%) and TBAH (1%), an entirely different absorption spectrum is obtained, and it is essentially the same as the one generated from the experiment described above in which a pyridine(98%)-TBAH(2%) solution was subjected to TCE vapor. Addition of 0.5 µL of neat TCE to a 3-mL solution of pyridine (99%) and TBAH (1%) caused the rapid development of a single intense absorbance at 418 nm (Figure 12). The exact absorptivities of the 550- and 418-nm bands were not measured; however, they seemed to be within an order of magnitude of each other. The 418 nm-band that developed using the 1% TBAH solution is probably the same as the 413 nm-band that develops in the 2% TBAH solution that was exposed to TCE vapor. Solvent effects may be the cause of the slight difference in the position of the peak maxima. If it assumed that these two bands are the same, the decay of absorbance signal is nearly a factor of three faster in the 2% TBAH solution than in the 1% mixture (Figure 13). The fact that the 413-nm band of the pyridine (99%)-TBAH (1%) solution does not appear simultaneous with the disappearance of the 550-nm absorption band indicates that the compounds that give rise to these two absorbances do not belong to a common reaction pathway.

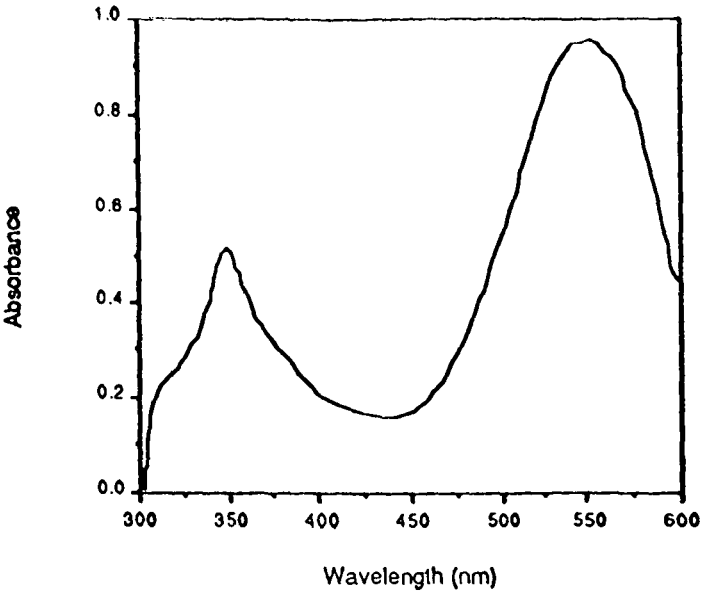

Figure 10. Absorption spectrum resulting from the reaction of neat trichloroethylene (TCE) with a solution of pyridine (90%), water (9%), and tetrabutylammonium hydroxide (TBAH) (1%).

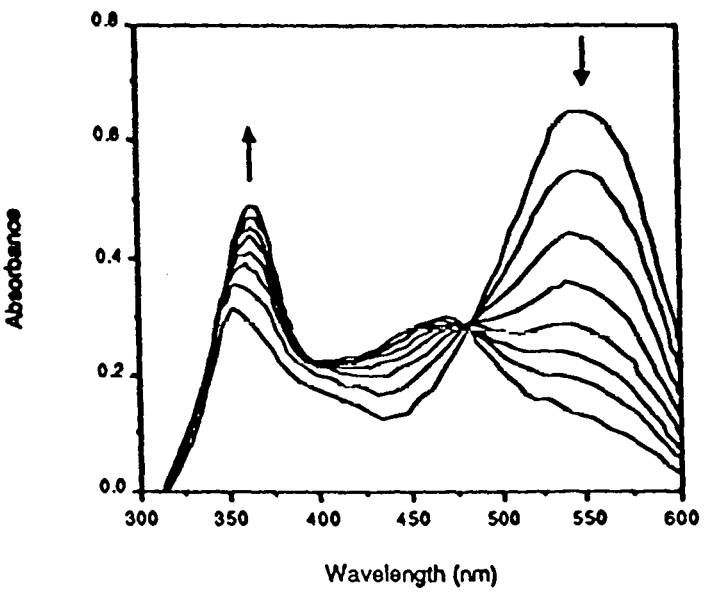

Figure 11. Degradation of the 550-nm band formed from the reaction of neat trichloroethylene (TCE) with a solution of pyridine (90%), water (9%), and tetrabutylammonium hydroxide (TBAH) (1%).

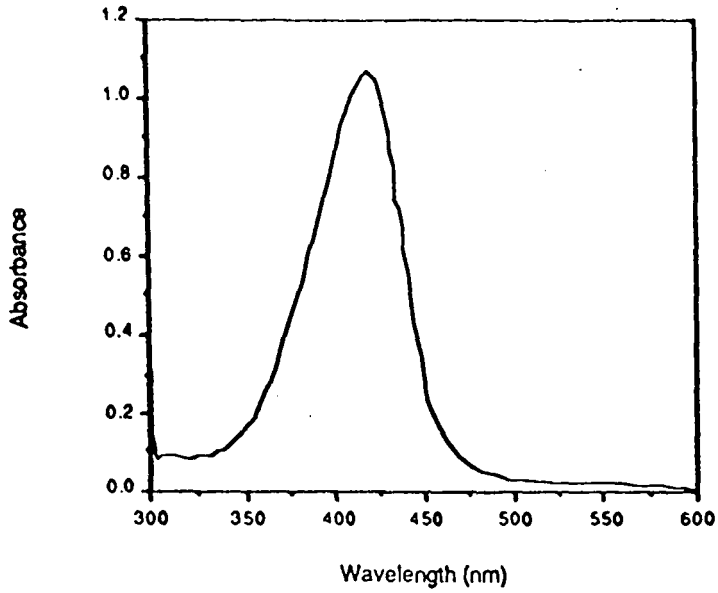

Figure 12. Absorption spectrum resulting from the reaction of neat trichloroethylene (TCE) with a solution of pyridine (99%) and tetrabutylammonium hydroxide (TBAH) (1%).

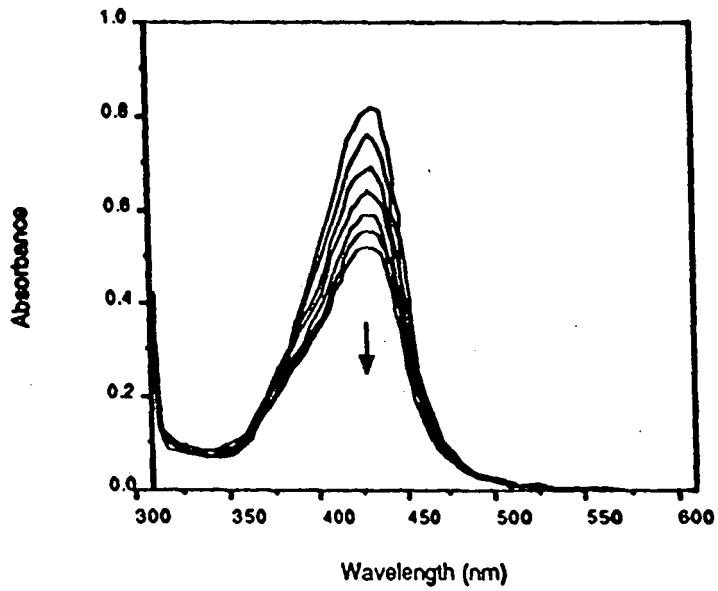

Figure 13. Degradation of the 418-nm band formed from the reaction of neat trichloroethylene (TCE) with a solution of pyridine (99%) and tetrabutylammonium hydroxide (TBAH) (1%).

We also examined the reaction of $CHCl_3$ with the "wet" and "dry" pyridine-TBAH solutions under conditions similar to the reactions with TCE. Addition of 0.2 µL of $CHCl_3$ to a 3-mL solution of pyridine (99%) and TBAH (1%) produced the spectra shown in Figure 14 with absorbance maxima at 368 and 404-nm. Once fully developed, the intensity of the absorbance did not change over a period of 1 hour. Addition of $CHCl_3$ to the "wet" solution of pyridine (90%)-TBAH (1%)-water (9%) gave the spectra shown in Figure 15. The simultaneous increase of the two absorbances at 367 and 532 nm indicates that they originate from the same molecule and are not the result of two competing processes. As in the reactions with TCE, the longer wavelength bands develop over a substantially longer period than the shorter wavelength absorbances. Development of the 404-nm band in the "dry" pyridine solution required only a few minutes, while the formation of the 532-nm absorbance occurred over a period of an hour.

These results clearly indicate that water plays a key role in the development of color in the TCE optrode. They also make it clear why the TCE-transmission curves plotted versus exposure time look qualitatively different than the $CHCl_3$ curves. It is likely that improved optrode response will result from making the TCE measurements while measuring at one of the isosbestic wavelengths mentioned above.

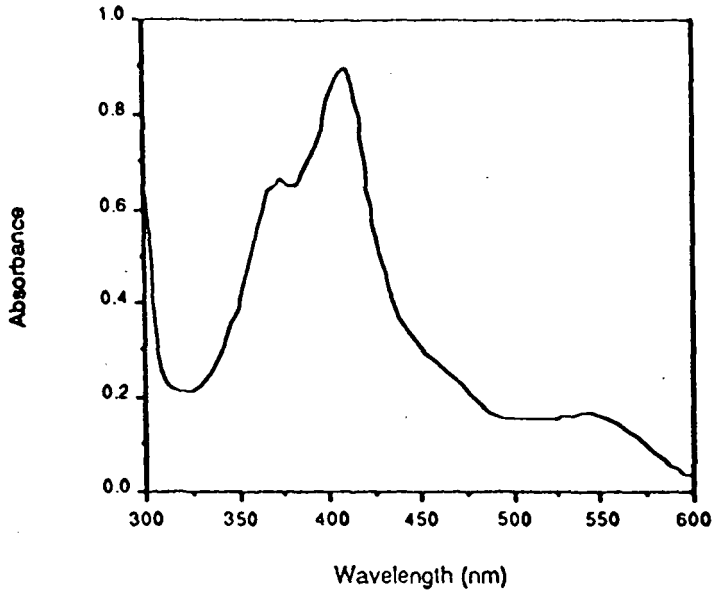

Figure 14. Absorption spectrum resulting from the reaction of neat chloroform ($CHCl_3$) with a solution of pyridine (99%) and tetrabutylammonium hydroxide (TBAH) (1%).

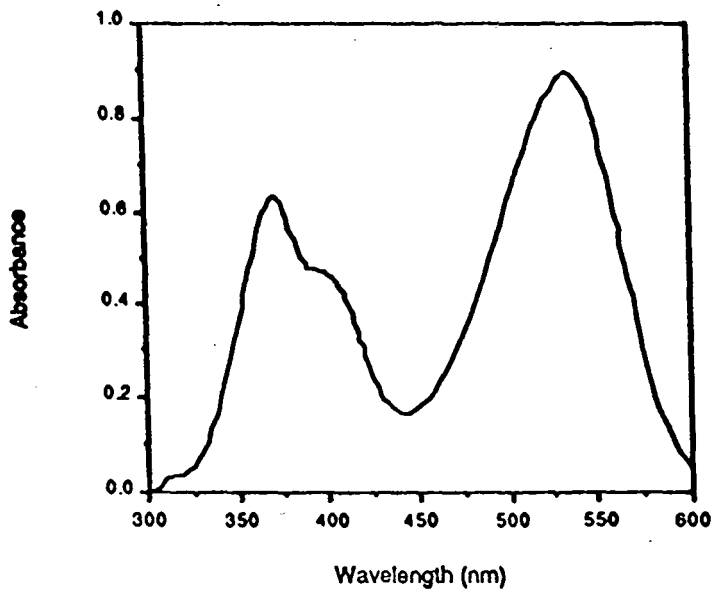

Figure 15. Absorption spectrum resulting from the reaction of neat chloroform ($CHCl_3$) with a solution of pyridine (90%), water (9%), and tetrabutylammonium hydroxide (TBAH) (1%).

2.3 FLUORESCENCE-BASED OPTRODES FOR TRICHLOROETHYLENE AND CHLOROFORM

We reported earlier that both TCE and $CHCl_3$ react under basic conditions with nonfluorescent 2-aminomethylpyridine (AMP, 8) to form highly fluorescent imidazopyridine derivatives.[15] Chloroform reacts with AMP to form the parent imidazopyridine (9), and we postulated that this reaction proceeds with the initial base-induced formation of dichlorocarbene ($:CCl_2$, 10). Subsequent reaction of the reactive divalent intermediate 10 with AMP generates the cyclic amidine 9. TCE also reacts under basic conditions

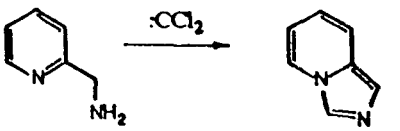

8 9

with AMP to form the imidazo lumophore; however, the reaction of the chlorinated olefin produced two fluorescent compounds.

In the presence of strong bases, TCE undergoes dehydrohalogenation forming DCA. This electrophilic alkyne is explosive in air, but is apparently stabilized by ether solvents and can even be co-distilled with diethyl ether in the absence of oxygen. DCA, generated from TCE in ether solutions containing alkylammonium hydroxides, reacts with AMP to form 11 and 12. From the distribution of products, we postulated that DCA reacts with AMP to initially afford 3-(chloromethyl)imidazopyridine (13). The benzyl-like 3-chloromethyl group on 13 most likely undergoes rapid substitution with AMP to form the secondary amine, 11. Subsequent reaction of 11 with another equivalent of 13 produces the second fluorescent product, 12, which contains two fluorescent moieties.

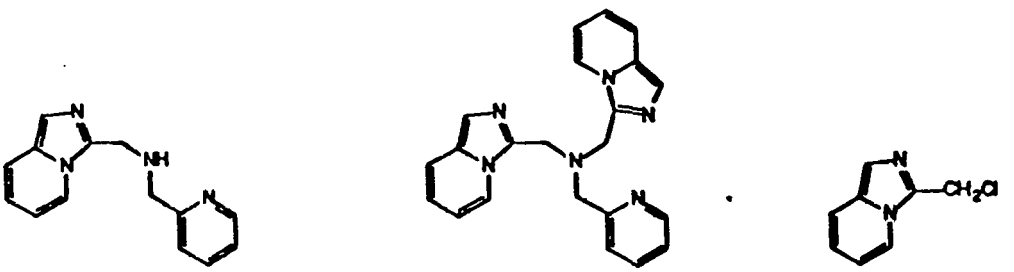

11 12 13

The initial work to evaluate the formation of the fluorescent products from $CHCl_3$ and TCE was performed in standard two-phase reaction media composed of an inert organic layer and a much denser aqueous phase containing 40% by weight sodium hydroxide. The organic layer contained the organohalide, AMP, and a tetraalkylammonium hydroxide phase-transfer catalyst. Conducting the reaction in this way

provided sufficient material to evaluate the reaction pathway and to identify the reaction products. However, earlier work by others found that two-phase reagent systems did not work well in optrodes because of the disparity in the densities of the immiscible aqueous and organic layers. Consequently, in our optrodes we employed a single-phase solution of indicator chemistry that consisted of TEGD as the solvent, AMP, and a commercially available 40% by weight aqueous solution of benzyltrimethylammonium hydroxide (BAH). The large alkyl groups of the ammonium counter ion help make the hydroxide soluble in the nonpolar ether solvent.

Figure 16 shows the response to TCE of a two-fiber fluorescence-based optrode filled with the single phase reagent. The optrode is an integrating sensor, and the concentration of analyte is a direct measure of the rate at which the fluorescence intensity increases. We have not determined the rate-limiting step for production of the fluorophore, however, both diffusion of the contaminant to the optrode and the conversion of TCE into the fluorescent product are concentration-dependent processes. As long as the optrode dimensions and reagent composition remain the same, the rate of fluorescence increase should be linearly related to the concentration of the contaminant. The data in Figure 17, which shows the rate of fluorescence increase as a function of TCE concentration, provide some indication that this is the case. These initial results were encouraging to us because, without much effort directed at probe development, we could already detect parts-per-million levels of TCE. However, further attempts to lower the detection limits and improve the response of the optrode proved difficult, and we began to suspect that fluorescence-based measurement may not afford the most sensitive detection method. So, in addition to fully characterizing the fluorescence-based optrode, we also made parallel efforts to develop an alternative sensor.

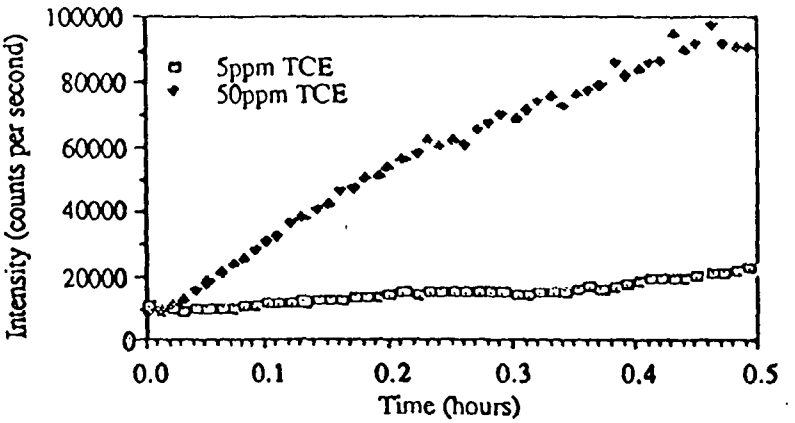

Figure 16. Fluorescence optrode timed response to two concentrations of trichloroethylene (TCE).

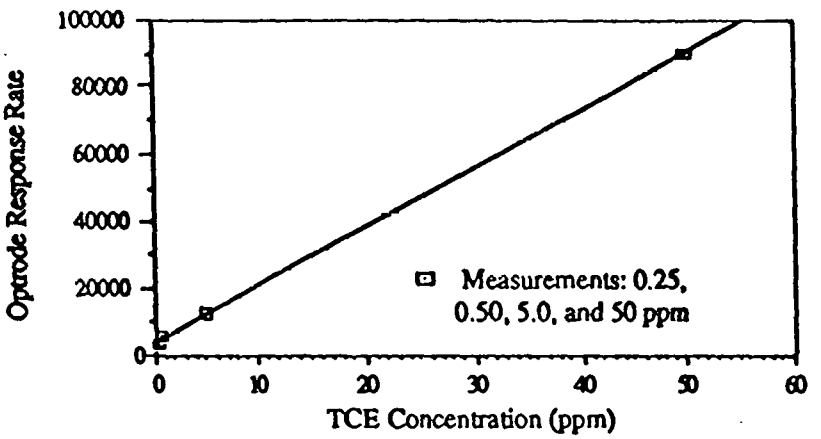

Figure 17. Response rate of fluorescence optrode at different trichloroethylene (TCE) concentrations.

2.4 EVALUATION OF THE FLUORESCENCE-BASED OPTRODE

The original single-phase optrode reagent used to produce the results in Figure 11 consisted of TEGD (47.5%), BAH (47.5%), and AMP (5%). However, commercially available BAH is contaminated with a potential inhibitor of lumophore synthesis, so we investigated other bases and reagent mixtures to improve the optrode detection limits. We examined the alkylammonium hydroxides listed below that can be obtained from commercial vendors:

tetramethylammonium hydroxide	pentahydrate	solid
tetraethylammonium hydroxide	40% in water	2.7 Molar
tetrapropylammonium hydroxide	20% in water	1.0 Molar
tetrabutylammonium hydroxide	40% in water	1.5 Molar

Of these bases, the tetrabutylammonium hydroxide solution provided the reagent system with the best overall response to TCE. The solid tetramethylammonium hydroxide was not soluble in the inert ether solvents, and the aqueous solution of tetraethylammonium hydroxide was apparently so polar that it was not miscible. The tetrapropyl solution was miscible, but reagent mixtures with this base did not respond well to TCE. We also tested a solution composed of just an alkylammonium hydroxide and AMP to determine if the ether co-solvent were actually required, and found we could not detect any fluorescence upon exposure of the probe to an aqueous 50-ppm TCE solution. In fact, the reagent media that produced the highest fluorescence levels were those prepared as dilute ether solutions of AMP and TBAH (TBAH refers to the commercially available 40% tetrabutylammonium hydroxide aqueous solution). Mixtures with various ratios of TBAH, AMP, and TEGD were evaluated, and the solution that produced the best response to TCE contained 5% AMP and 10% TBAH. Although other ethers of ethylene glycol homologs are available, the low vapor pressure and solvation properties of TEGD made this solvent nearly ideal for our application.

The conversion of TCE into DCA and the subsequent reactions to form the fluorescent indicator product consumes, for a stoichiometric reaction, three equivalents of hydroxide for each lumophore produced. Because the optrode contains only a few microliters of indicator solution, we were concerned that the response of an optrode may be affected by the consumption of reagents during the normal course of a measurement. Therefore, we used radioactive ^{14}C-labeled TCE to determine the amount of TCE absorbed by the optrode during a normal measurement. A standard measurement was performed with radiolabeled TCE-contaminated water, and at the end of the test the optrode reagent was transferred to a scintillation counter which determined the amount of TCE absorbed by the probe. Results showed that 0.087 µg of TCE per 1.0 µL of indicator solution was absorbed from water contaminated with 10 ppm of TCE. The data in Table 1

indicate that at the given reagent concentrations, only about 1% of the total base is consumed (2.0×10^{-9} moles), and this amount would probably not be enough to alter the response rate of the probe, even if it were to be a reaction-limited response.

Table 1. Reagent composition of fluorescence optrode indicator solution.

Reagent	% of solution	µg/µL	moles
TEGD	85	850	--
AMP	10	100	4.6×10^{-7}
TBAH	5	50	1.5×10^{-7}
TCE	--	0.087	6.6×10^{-10}

With the indicator reagent and the chemistry of transduction mechanism reasonably well defined, we began to evaluate the response of the optrode to various concentrations of TCE-contaminated water. However, almost immediately we found that we could not obtain reproducible responses to identical concentrations of TCE. We focused our attention on the indicator chemistry because it was noticed that, as these solutions aged, they began to discolor. Generally, the indicator solutions were mixed just before preparing an optrode for evaluation, but indicator solutions just a few hours old did not produce the same level of fluorescence as the freshly made material.

The optical absorbances of the individual components of the indicator solution were measured with a Vis spectrophotometer, and none of the reagents exhibited an appreciable absorbance above 340 nm. Neat reagent-grade AMP develops a light yellow color as it ages, but the color is removed by distillation. TEGD and the aqueous solution of TBAH did not develop any discoloration while kept in their original containers. However, the addition of TBAH to a nondistilled volume of TEGD caused the resulting mixture to develop a deep amber color over a period of just 20 min. As seen in Figure 18, the transmittance (absorbance = log (1/transmittance) of the ether at 350 nm is greater than 95%, but upon addition of TBAH the transmittance drops immediately to about 15% and finally reaches a minimum of 6% after 20 min. The subsequent addition of AMP does not substantially diminish the solution transmittance. Obviously a reaction occurs between the ether and base. Ethers are known to form hydroperoxides readily on exposure to air, and, in the presence of base, these compounds decompose, yielding a variety of chain-shortened products. Hydroperoxides also oxidize amines.

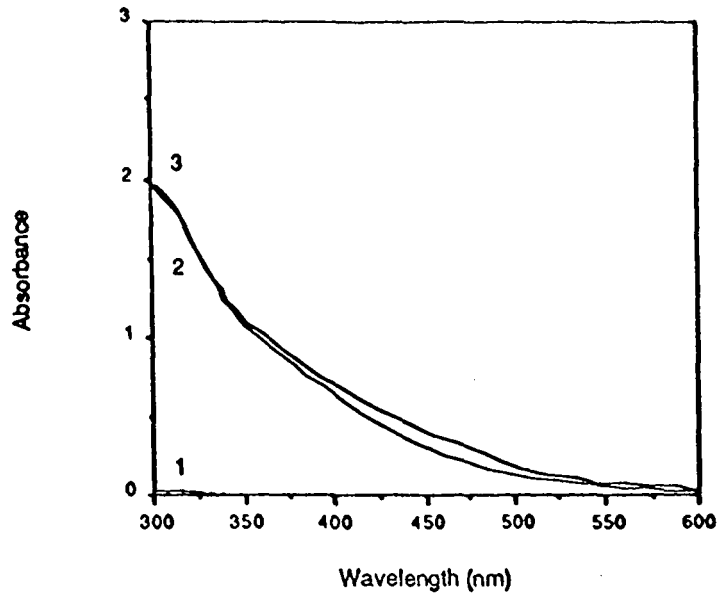

Figure 18. Absorption spectra of (1) nondistilled tetraethyleneglycol dimethyl ether (TEGD) (baseline) (2) nondistilled TEGD (90%) with tetrabutylammonium hydroxide (TBAH) (10%) and (3) nondistilled TEGD (85%), TBAH (10%), and nondistilled aminomethylpyridine (AMP)(5%).

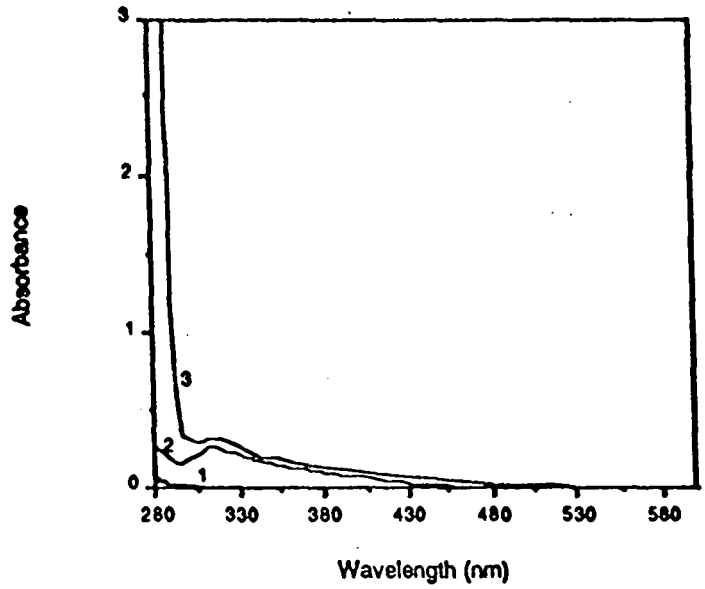

Figure 19. Absorption spectra of (1) distilled tetraethyleneglycol dimethyl ether (TEGD) (baseline) (2) distilled TEGD (90%) with tetrabutylammonium hydroxide (TBAH) (10%) and (3) distilled TEGD (85%), TBAH (10%), and distilled aminomethylpyridine (AMP) (5%).

Consequently, the ether was distilled. Nevertheless, addition of TBAH to the purified ether still resulted in the production of a broad absorbance near 350 nm. However, the solution transmittance was greater than 70% (Figure 19), a marked improvement over the nondistilled reagent. Because the intensity of the fluorescence emission is directly proportional to the intensity of incident light, the formation of species that absorb light in the spectral region of the lumophore excitation band will have a pronounced effect on the accuracy of the optrode.

We examined the effect that the discoloration of the indicator reagent has on the fluorescence emission intensity by performing a series of experiments under controlled conditions in a fluorimeter. The optrode was not used because of a concern that it might provide some anomalous contributions to overall results. Sample solutions were illuminated with 365-nm light emitted by a mercury-vapor lamp. The source emission was passed through a monochromator, and the selected band of light was focused on a cuvette. Right-angle fluorescence emission was collimated and focused into a second scanning monochromator. Interference from scattered exciting light was eliminated with a 350-nm long-pass filter installed between the cuvette and the emission monochromater.

The fluorescence emission from distilled and nondistilled TEGD, and mixtures made from the subsequent addition of TBAH and AMP, are shown in Figures 20 and 21. Neat TEGD, nondistilled and distilled, provided only low-level background signals. However, addition of TBAH produced a substantial increase in the fluorescence signals from both mixtures, although the emission intensity from the solution of the nondistilled ether was almost five times that of the solution made with the distilled solvent. Adding AMP to the solution of distilled TEGD and TBAH caused only a modest increase in signal. Curiously, the addition of AMP to the solution of nondistilled TEGD reduced the emission intensity by nearly 30%. However, the absorption of the incident 365- nm light could easily be seen as it passed through the yellowish indicator reagent prepared from nondistilled ether.

Equal amounts of TCE were added to two indicator solutions (1 µL/mL), one prepared from newly purchased reagents (TEGD, AMP) and the other from these reagents freshly distilled. The reaction of TCE with AMP produced a concentration of lumophore so high in each solution that only front-face emission was detected. The solutions were then diluted with equal volumes of the corresponding indicator reagent to eliminate lumophore-induced inner-filter effects. The fluorescence emission spectra of these solutions are shown in Figures 22 and 23, with their indicator reagent backgrounds subtracted. The solution prepared with freshly

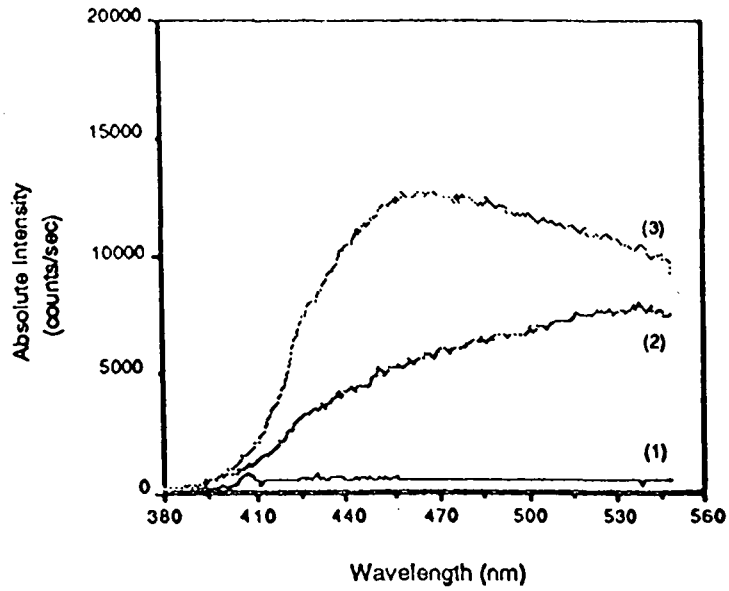

Figure 20. Fluorescence emission spectra of (1) nondistilled tetraethyleneglycol dimethyl ether (TEGD) (2) nondistilled TEGD (90%) with tetrabutylammonium hydroxide (TBAH) (10%) and nondistilled aminomethylpyridine (AMP) (5%) and (3) nondistilled TEGD (90%) with TBAH (10%).

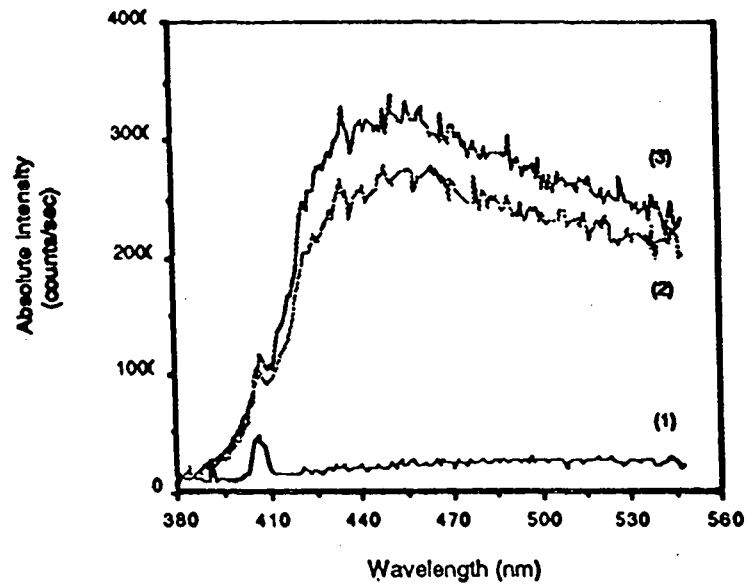

Figure 21. Fluorescence emission spectra of (1) distilled tetraethyleneglycol dimethyl ether (TEGD) (2) distilled TEGD (90%) with tetrabutylammonium hydroxide (TBAH) (10%) and (3) distilled TEGD (90%) with TBAH (10%) and distilled aminomethylpyridine (AMP) (5%).

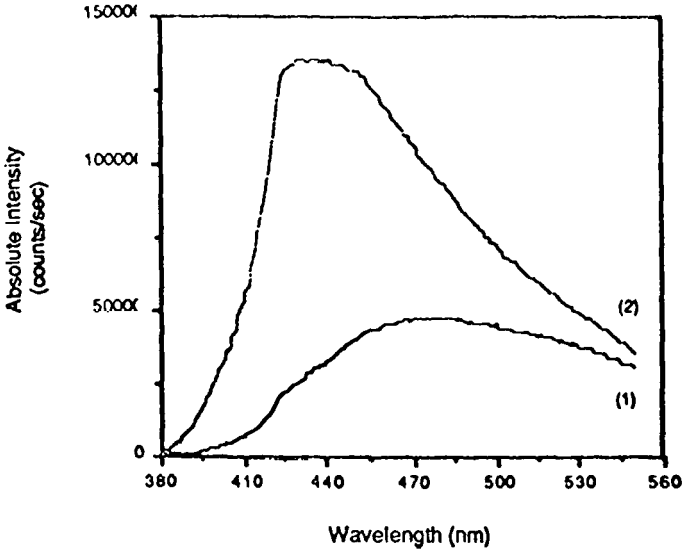

Figure 22. Absolute intensity of fluorescence emission spectra resulting from the addition of neat trichloroethylene (TCE) to solutions consisting of (1) nondistilled tetraethyleneglycol dimethyl ether (TEGD) (85%), tetrabutylammonium hydroxide (TBAH) (10%), and nondistilled aminomethylpyridine (AMP) (5%); (2) distilled TEGD (85%), TBAH (10%), and distilled AMP (5%).

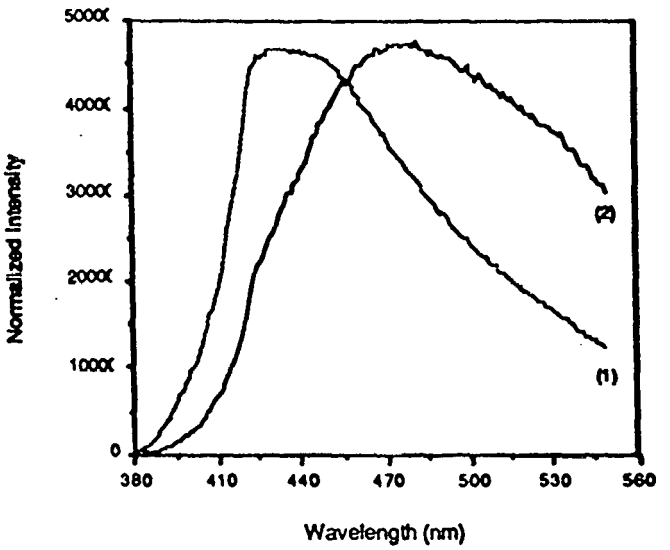

Figure 23. Normalized fluorescence emission spectra resulting from the addition of neat trichloroethylene (TCE) to solutions consisting of (1) nondistilled tetraethyleneglycol dimethyl ether (TEGD) (85%), tetrabutylammonium hydroxide (TBAH) (10%), and nondistilled aminomethylpyridine (AMP) (5%); (2) distilled TEGD (85%), TBAH (10%), and distilled AMP (5%).

distilled reagents produced a fluorescence signal nearly five times as intense as the indicator solution made with newly purchased reagents. Also, the emission peak maxima of the solution prepared with nondistilled ether exhibits a bathochromic shift of nearly 30 nm, while the emission derived from solutions of freshly purified TEGD and AMP was quite similar to the fluorescence spectra of the parent imidazopyridine derivatives (Figure 23).

Similar variable results were obtained with a two-fiber fluorescence optrode excited with the 10-nm wide 355-nm emission of a Coherent Innova 90 argon-ion laser operated. The light from the laser was launched into a 200-μm-diam core glass-on-glass Diaguide optical fiber that was connected to a 1-mm diam capillary tube, 6 mm in length, opened at the opposite end (see Figure 24). A second adjacent and parallel fiber was used to collect the fluorescence emission and

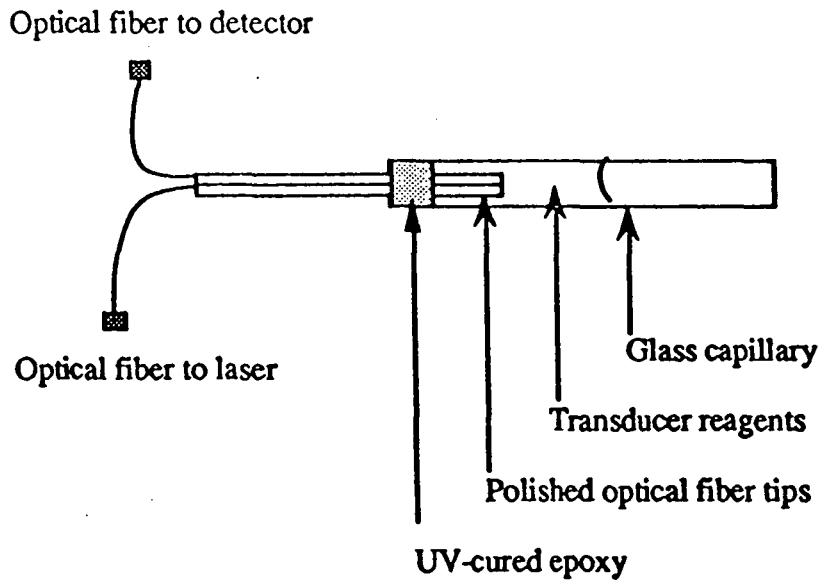

Figure 24. Diagram of a two-fiber fluorescence optrode.

to direct this light to a scanning monochromator. The optrode, filled with a measured volume of reagent (between 5 and 10 μL), was exposed to head-space vapor that emanated from water containing 10 ppm of TCE. Despite many attempts, we were unable to obtain results that could be reproduced. In addition to large background signals of variable intensity (Figures 25 and 26), the probes did not respond in comparable magnitude to equal concentrations of analyte. Clearly, the failure to obtain consistent results arose from the instability of the indicator reagent and its individual components. Because of these difficulties, we directed

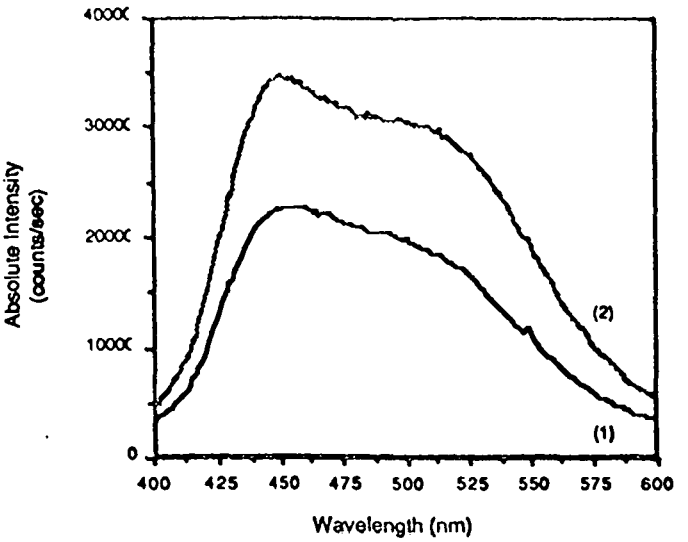

Figure 25. Absolute fluorescence emission intensity measured through a two-fiber optrode containing a solution of (1) nondistilled tetraethyleneglycol dimethyl ether (TEGD) (85%), tetrabutylammonium hydroxide (TBAH) (10%), and distilled aminomethylpyridine (AMP) (5%); (2) solution in (1) exposed to head-space vapor from aqueous 5-ppm trichloroethylene (TCE) solution.

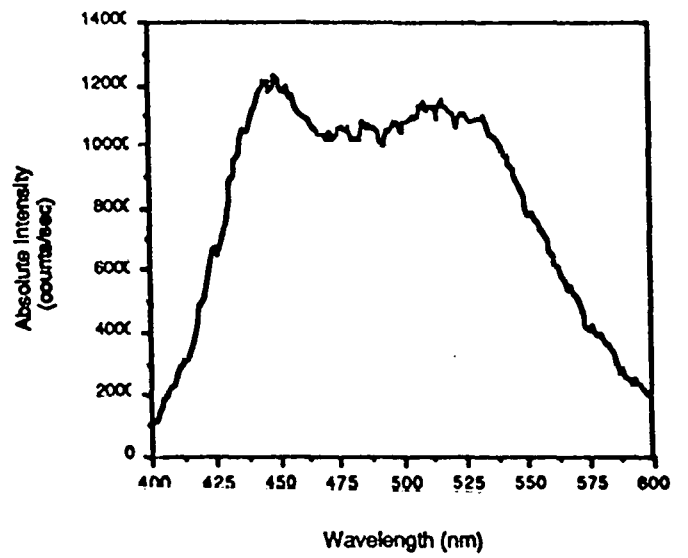

Figure 26. Fluorescence emission through a two-fiber optrode containing indicator reagent [nondistilled tetraethyleneglycol dimethyl ether (TEGD) (85%), tetrabutylammonium hydroxide (TBAH) (10%), and distilled aminomethylpyridine (AMP) (5%)] exposed to head-space vapor from aqueous 5-ppm trichloroethylene (TCE) solution. Background of indicator reagent has been subtracted from total solution fluorescence.

our efforts toward a new probe design that exploits the optical transmittal of a different indicator reagent (absorption optrode described in Section 2). This new probe design is not influenced by many of the factors that we found that drastically affected the results of the fluorescence-based optrode. The success of the absorption optrode makes it no longer necessary to continue to improve the fluorescence-based optrode. However, the knowledge gained in investigating the latter should be very useful in designing future optrodes.

3. CONCLUSIONS

This report describes and evaluates a new absorption-based fiber-optic chemical sensor (optrode) for selective determination of trichloroethylene (TCE) and chloroform ($CHCl_3$) in groundwater. The sensor is sensitive to TCE and $CHCl_3$ below 10 ppb and has high accuracy. The device is based on a colorimetric indicator that turns red in the presence of even trace amounts of these two chemicals. The amount of red color that develops in the optrode after exposure to the chemical is linearly related to the concentration of the chemical. The use of fiber optics to interrogate the device results in a remote *in situ* sensor. The optrode does not respond to similar chlorinated hydrocarbons commonly found with TCE and $CHCl_3$ in contaminated wells.

The chemical behavior of chlorinated hydrocarbons, specifically TCE and $CHCl_3$, are reported, in terms of designing fluorescence- and colorimetric-based optrodes. These studies provided the insight that led to the success of the absorption optrode. This work will also be valuable in the design of future optrodes. One promising chemistry-based method exploits the formation of a charge-transfer complex formed between triphenylphosphine (Ph_3P) and carbon tetrachloride (CCl_4) and the reactivity of this complex toward N-alkylated formamides. We will attempt to incorporate this reaction into an optrode to allow the measurement of CCl_4 in groundwater and wastewater. Perchloroethylene ($Cl_2C{=}CCl_2$) is also a groundwater contaminant found at many Department of Energy sites. This organohalide is an electron-deficient olefin and is an efficient fluorescence quencher. The ability of $Cl_2C{=}CCl_2$ to quench fluorescence indicates that a fiber-optic sensor that exploits this behavior could be developed. Because $Cl_2C{=}CCl_2$ quenches fluorescence in a way that does not involve a chemical reaction, a reversible optrode could be developed to allow continuous long-term monitoring of this haloalkene.

4. RECOMMENDATIONS

4.1 FUTURE ORGANOCHLORIDE OPTRODE RESEARCH

The performance of the colorimetric organochloride optrode is sufficient for many applications. We are currently evaluating its use in monitoring microbial degradation of selected environmental contaminants. For example, some microbes can degrade carbon tetrachloride (CCl_4) to chloroform ($CHCl_3$) under anaerobic conditions and are being selected for remediation of contaminated aquifers. We are using the $CHCl_3$ optrode to monitor its rate of microbial degradation in laboratory microcosms in hopes of using this technique to monitor microbial degradation remotely *in situ* in aquifers in the future.

In late 1989, we will begin evaluating the use of the trichloroethylene (TCE) optrode to measure TCE vapors in contaminated soils at Lawrence Livermore National Laboratory (LLNL). This work is funded as a Hazardous Waste Remedial Action Program (HAZWRAP) Demonstration Phase project. Initially, the optrode will be used in combination with other techniques. However, eventually we would like to use the optrode for rapid screening of subsurface contaminants. Toward this purpose, we are developing a portable instrument that uses light-emitting diodes as the light source. Not only will such revisions make the instrument smaller but it should also improve the precision of our measurements because of the stability of light-emitting diode sources.[16]

4.2 NEW FIBER-OPTIC BASED SENSORS (OPTRODES)

Beginning in FY 1990, the research phase of this project will be directed toward developing new optrodes. During that year we will select one or two target contaminants and design specific optrodes for those contaminants. The selection will be based on DOE community need and the feasibility of developing the optrode in a reasonable period (2 years). Some preliminary work was done in FY 1989, and a few potential contaminants and indicator chemistries were identified.

4.2.1. Carbon Tetrachloride

We are presently investigating a fiber-optic method for measuring the concentration of aqueous CCl_4. One promising chemistry-based method exploits the formation of a charge-transfer complex formed between triphenylphosphine (Ph_3P) and CCl_4 and the reactivity of this complex toward N-alkylated formamides. We coupled the chemical activity of these reagents and developed a high-yield reaction that forms intensely fluorescent products from CCl_4. This reaction will

be incorporated into an optrode to allow the measurement of CCl_4 in groundwater and wastewater.

The initial formation of the Ph_3P-CCl_4 complex can be used to develop colorimetric tests for CCl_4 in a manner analogous to the formation of fluorescent compounds. In this way, the colorimetric CCl_4 indicator can be used with the existing TCE optrode system with minor modifications. Additionally, the complex may be of value in creating nonoptical methods for measuring this organohalide. These additional techniques would be based on the ionic nature of the phosphorous-organohalide interaction and might involve the use of ion-selective field effect transistors, ion-selective electrodes, or surface-acoustic-wave devices.

4.2.2. Perchloroethylene

Perchloroethylene ($Cl_2C=CCl_2$) is a groundwater contaminant found at many Department of Energy sites. This organohalide is an electron-deficient olefin and is an efficient fluorescence quencher. The ability of $Cl_2C=CCl_2$ to quench fluorescence indicates that a fiber-optic sensor that exploits this behavior could be developed. Because $Cl_2C=CCl_2$ quenches fluorescence in a way that does not involve a chemical reaction, a reversible optrode could be developed to allow continuous long-term monitoring of this haloalkene.

4.2.3. Polynuclear Aromatic Compounds

It was recently reported that water-soluble cyclophanes were shown to reversibly bind pyrene dissolved in aqueous solutions. The binding of organic molecules by cyclophanes is not unique; however, the development of cyclophanes with cationic ammonium groups that allow these large organic molecules to be soluble in water is noteworthy. The construction of specially designed cyclophanes should allow the development of optical sensors that could be targeted to specific polynuclear aromatic compounds (PNAs). Cyclophanes are composed of two aromatic molecules bonded together by short alkyl chains to form ring-like structures. The hole within the ring is determined by the size of the aromatic groups and the lengths of the alkyl linkages. Large aromatic groups with long chains provide ring structures with large centers. Conversely, smaller side chains and aryl groups produce cyclophanes with smaller diameter holes. Cyclophanes could thereby be prepared that would possess centers of the appropriate size to bind specific molecules reversibly. The transduction of the binding event can be measured optically in either of two ways: (1) by measurement of the fluorescence emission of an eximer formed by the cyclophane and targeted PNA, or (2) by colorimetric detection of a ground state charge-transfer complex formed between the specific groundwater PNA contaminant and the cyclophane. The adaption

of cyclophanes to fiber optics would provide a reversible, optically based sensor for measuring PNAs in groundwater.

Although the use of cyclophanes represents a very highly selective method for discriminating between various PNAs, the formation of charge-transfer complexes with other donor/acceptor counterparts would provide a more simplified, but less specific, colorimetric scheme for detecting PNAs.

4.2.4. Heavy Metals (Chromium and Uranium)

Chromium and uranium are metals that exhibit photophysical properties that will allow them to be detected optically by fiber-optic sensors. Chromium, and its complexes, have distinct optical absorptions in the visible spectrum; however, because the absorptivity of these complexes is generally low, sensitive determination of the ion concentration is not possible. The use of ion-sequestering agents, such as crown ethers and various organic polymers, can be exploited to concentrate the chromium ion to allow real-time *in situ* optical measurement of its concentration in groundwater. Similarly, the inherent fluorescent characteristics of uranium (UO_2^{+2}) might be used to develop fiber-optic sensors for this element.

REFERENCES

1. Seitz, W.R.; "Chemical Sensors Based on Fiber Optics," *Anal. Chem.* **1984**, *56*, 16A.

2. Wolfbeis, O.S.; "Fluorescence Optical Sensors in Analytical Chemistry," *Trends in Analytical Chemistry* **1985**, *4*, 184.

3. Angel, S.M.; "Optrodes: Chemically Selective Fiber-Optic Sensors," *Spectroscopy* **1987**, *2*, 38.

4. Kulp, T.J.; Camins, I.; Angel, S.M.; Munkholm, C.; Walt, D.R.; "Polymer immobilized enzyme optrodes for the detection of penicillin," *Anal. Chem.* **1987**, *59*, 2849.

5. Angel, S.M.; "Development of Fiber Optics Sensors for Temperature Measurement and Chemical Analysis in Geothermal Wells," *Geothermal Resources Council, Transactions* **1987**, *11*, 155.

6. Angel, S.M.; Katz, L.F.; Archibald, D.D.; Lin, L.T.; Honigs, D.E.; "Near-Infrared Surface-Enhanced Raman Spectroscopy. Part I: Copper and Gold Electrodes," *Appl. Spectrosc.* **1988**, *42*, 1327.

7. Kulp, T.J.; Bishop, D.; Angel, S.M.; "Column-Profile Measurements Using Fiber-Optic Spectroscopy," *J.Soil Sci.Soc.Am.* **1988**, *52*, 624.

8. Milanovich, F.P.; Garvis, D.G.; Angel, S.M.; Klainer, S.K.; Eccles, L.; "Remote Detection of Organochlorides with a Fiber Optic Based Sensor," *Anal. Inst.* **1986**, *15*, 137.

9. Cowles, T.J.; Moum, J.N.; Desiderio, R.A.; Angel, S.M.; "In situ monitoring of ocean chlorophyll via laser-induced fluorescence backscattering through an optical fiber," *Appl. Optics* **1989**, *28*, 595.

10. Angel, S.M.; Garvis, D.G.; Sharma, S.K.; Seki, A.; "Field Applications of Fiber-Optic Sensors. Part I: Temperature Measurements in a Geothermal Well," *Appl. Spectrosc.* **1989**, *43*, 430.

11. Angel, S.M.; Daley, P.F.; Langry, K.C.; Albert, R.; Kulp, T.J.; Camins, I.; "The Feasibility of Using Fiber Optics for Monitoring Groundwater Contaminants IV. Mechanistic Evaluation of the Fujiwara Reaction for Detection of Organic Chlorides." Quarterly Technical Report, Contract No. AD-89-F-2A074, U.S. Environmental Protection Agency (June 18, 1987).

12. Uno, T.; Okumura, K.; Kuroda, Y.; "The Fujiwara Reaction: Isolation and Structural Investigation of the Reaction Product from Chlorofrom," *Chem. Pharm. Bull.* **1982**, *30*, 1876.

13. Reith, J.F.; van Ditmarsch, W.C.; de Ruiter, T.; "An Improved Procedure for Application of the Fujiwara Reaction in Determination of Organic Halides," *Analyst* **1974**, *99*, 652.

14. Kende, A.S.; Fludzinski, P.; "A Convenient Laboratory Synthesis of Dichloroacetylene," *Synthesis* **1982**, 455.

15. Angel, S.M.; Langry, K.C.; Kulp, T.J.; Daley, P.F.; Bishop, D.J.; "In Situ Detection of Organic Molecules," Annual Report, Contract No. DE-AC05-84OR21400, U.S. Department of Energy, Hazardous Waste Remedial Actions Program, **1988**.

16. Smith, B.W.; Jones, B.T.; Winefordner, J.D.; "High-Precision Fluorimetry with a Light-Emitting Diode Source," *Appl. Spectrosc.* **1988**, 42, 1469.

APPENDIX

The following text is taken from a paper that was recently submitted by Kevin Langry to the Journal of Organic Chemistry. It describes the chemistry of $CHCl_3$ with 2-(aminomethyl)pyridine and base and resulted from the work on the chloroform fluorescence- and absorption-based optrodes.

ABSTRACT

The reaction of chloroform with 2-(aminomethyl)pyridine under basic phase-transfer catalysis affords imidazo[1,5-a]pyridine in 26% isolated yield. Despite the formation of considerable tarry residue, gas chromatography indicates that the volatile fraction of the reaction is simple and consists of imidazo[1,5-a]pyridine and two minor components identified as N-(2-pyridyl-methyl)formamide and (2-pyridylmethyl)-isonitrile. The basic phase-transfer catalyzed reaction of chloroform with a series of α-(aminomethyl)azanaphthalenes was found to be general and yield the corresponding annulated imidazo derivatives: 2-(aminomethyl)quinoline yields imidazo[1,5-a]quinoline; 2-(aminomethyl)-4-methoxyquinoline yields 5-methoxyimidazo[1,5-a]quinoline; and 1-(aminomethyl)-isoquinoline yields imidazo[5,1-a]isoquinoline. However, 3-(aminomethyl)isoquinoline failed to provide any of the expected imidazo[5,1-b]isoquinoline. Despite product yields in the 25% range, GC of the reaction mixtures indicates that the volatile fractions generally consist of residual starting aminomethyl compound, the imidazo product, and a minor amount of the (α-azanaphthylmethyl)formamide.

BACKGROUND

Groundwater contaminated with $CHCl_3$ has become an important public health issue, and considerable effort is being directed toward development of low-cost on-site analytical methods for monitoring contamination levels. We sought to apply remote fiber fluorimetry[1] to groundwater analysis, and for this we needed to develop a sensitive fluorometric method capable of detecting micro- to nanomolar concentrations of $CHCl_3$ dissolved in water. In this report, we describe the reaction of $CHCl_3$ under basic phase-transfer catalysis (PTC) with 2-(aminomethyl)pyridyl derivatives to form intensely fluorescent imidazopyridines.

Our goal was to develop a simple, efficient, "one-pot" reaction that would generate fluorescent products from $CHCl_3$ and nonfluorescent precursors. The general approach we took was to incorporate the single carbon of $CHCl_3$ into a precursor in a manner that would create a luminescent product. The nonfluorescent 2-(aminomethyl)pyridine (2-AMP, **1**) was selected as the precursor because this substrate, with the addition of a single carbon species, could potentially be converted into the highly fluorescent imidazo[1,5-a]pyridine (**2**, eq. 1).[2]

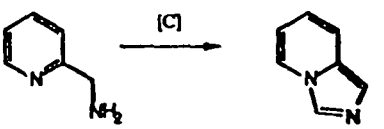

eq. 1

1 **2**

The proposed conversion of **1** into the bicyclic amidine **2**, outlined in eq. 1, is modeled after the reaction of 2-AMP with formic acid and phosphorous oxychloride ($POCl_3$).[3] As shown in eq. 2, following formation of the formamide **3** from 2-AMP and formic acid, treatment of **3** with $POCl_3$ yields the imidazopyridine **2**. Undoubtedly, the reaction of the amide **3** with $POCl_3$ involves formation of the iminium ion **4**.[4] The proximity of the nucleophilic pyridyl nitrogen to the electrophilic chloromethyleniminium carbon promotes an intramolecular ring closure that subsequently leads to formation of the bicyclic imidazopyridine **2**.

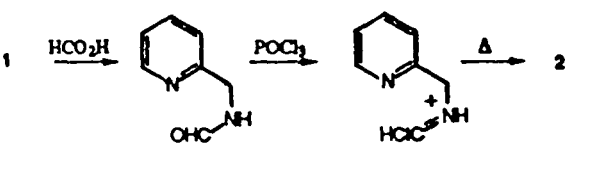

eq. 2

3 **4**

Unfortunately, $CHCl_3$ is not sufficiently reactive toward nucleophilic amines[5] to allow the aminomethyl group of **1** to facilitate formation of the imidazopyridyl system. However, $CHCl_3$ undergoes facile dehydrohalogenation in the presence of hydroxide ions to generate dichlorocarbene ($:CCl_2$),[6] and this reactive divalent carbon species has been shown to combine with primary amines to form isonitriles.[7] The formation of isonitriles from mixtures of $CHCl_3$, alkaline hydroxide, and primary amines is postulated to proceed by way of a chloromethylenimine intermediate that subsequently experiences a-dehydro-halogenation to form an isonitrile (eq. 3).

$$R\text{-}NH_2 \longrightarrow R\text{-}\overset{+}{N}H_2\text{-}\overset{-}{C}Cl_2 \longrightarrow R\text{-}NH\text{-}CHCl_2 \longrightarrow R\text{-}\overset{+}{N}H{=}CHCl \longrightarrow R\text{-}\ddot{N}C: \qquad \text{eq. 3}$$

It was our intent to generate the fluorescent imidazopyridyl structure with $CHCl_3$ by exploiting the putative intermediacy of the carbene-derived chloromethylenimine moiety. Formation of this electrophilic imine from the primary amine of 2-AMP should promote an intramolecular cyclization reaction analogous to the $POCl_3$-induced ring closure depicted in eq. 2.

Results and Discussion

The reaction of 2-AMP in 1,2-dimethoxyethane (DME) with $CHCl_3$ and tetrapropylammonium bromide stirred over 40% aqueous NaOH at 55°C provided, along with considerable tar-like residue, the expected imidazo[1,5-a]pyridine (**2**) in 26% isolated yield. Because **2** discolors in air, purification of the imidazopyridine was best achieved by column chromatography of the crude reaction extract, followed by condensation of the product residue onto a cold finger at reduced pressure. Despite the condition of the final reaction mixture and the relatively poor yield, the intense fluorescence of **2** (excitation at 254 nm or 366 nm, emission λ_{max} 447 nm) allowed the initial progress of the reaction to be easily monitored by analytical thin layer chromatography (TLC).

Clearly, the low product yield suggests that the reaction of $:CCl_2$ with **1** does not follow a single pathway. In addition to the aminomethyl group, the pyridyl ring nitrogen is also a potential site for reaction with $:CCl_2$. Scheme I presents the most probable paths available to the reaction of 2-AMP with $CHCl_3$ under basic PTC.

Path *a* of Scheme I is consistent with the generally accepted sequence for the reaction of $:CCl_2$ with primary amines; however, this progression of intermediates avails

itself to a variety of potentially isolable reaction products.[7a] In this sequence and subsequent to the formation of zwitterion **5**, hydrolysis of either the dichloromethylamine **6** or the ensuing chloromethylenimium ion **4** would yield N-(2-pyridylmethyl)formamide (**3**).[8a] Thereafter, **4** can undergo ring closure and form the imidazopyridine, or it can suffer a-dehydrochlorination to provide the corresponding isonitrile (**7**).

Analysis by GC-mass spectrometry (MS) of the organic phase from the reaction of 2-AMP with $CHCl_3$ indicated that the volatile fraction of the reaction mixture was not very complex. In addition to **1** and **2**, the only other principal components were a minor fraction (<3%) that exhibited a molecular ion of *m/z* 136 and a fourth fraction that provided a molecular ion of *m/z* 118. The GC retention time and MS fragmentation pattern of the compound with *m/z* 136 were consistent with data obtained from an authentic sample of formamide **3**.[3] However, the quantity of **3** detected in the mixture was not representative of the actual amount produced during the reaction. Control reactions show that, under the basic PTC conditions, the formamide is cleanly and rapidly hydrolyzed to **1**, with a reaction half-life of about 55 min.

The existence of a second component with *m/z* 118 and the presence of a faint pungent odor that emanated from the reaction mixture suggested that (2-pyridylmethyl)-isonitrile (**7**) was also formed. The GC retention times for **2** and **7** on a DB1 capillary column were quite distinct, with the more mobile isonitrile fraction eluting the column first. The MS fragmentation patterns for the two compounds were remarkably similar, except for a consistent difference in the ratios of the fragment ion intensities: **2** *m/z*(%) 118(100), 92(22), 78(17), 64(40); **7** *m/z*(%) 118(100), 92(20), 78(94), 64(26).

When we monitored the course of the reaction by GC, we found an initial commensurate production of both **2** and **7**, although the isonitrile was generally never greater than about 15% of the imidazopyridine. However, as the reaction time increased, the intensity of the isonitrile diminished until none could be detected. The loss of **7** may result from a number of reactions. Generally, the formation of isonitriles with $CHCl_3$ and alkaline hydroxide is not very efficient and often results in the production of tars, especially when other functional groups are present that can compete for the carbene.[8] Because the chloromethyleniminium ion is a putative intermediate common to both isonitrile formation and the proposed imidazo ring closure, we wanted to be assured that isonitriles could in fact be derived from (aminomethyl)pyridines under our PTC conditions. Therefore, 3-(aminomethyl)pyridine (**9**) was treated with $CHCl_3$ under PTC conditions with sodium hydroxide solution. Although the reaction produced a great deal of insoluble material, the (3-

pyridylmethyl)isonitrile (10) (R-NC n 1652 cm^{-1})[9] was isolated by distillation in 20% yield.

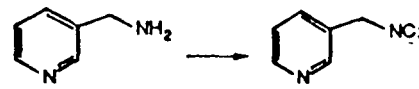

eq. 4

9 10

To measure directly the chemistry of **7** under the PTC conditions that we have used, we attempted to prepare the isonitrile employing the method developed by Appel and co-workers.[10] It has been shown that, with (2-pyridylmethyl)formamide, this procedure gives both **2** (30%) and **7** (70%).[9] Our attempt with this reaction gave, by GC-MS analysis, nearly equal amounts of **2** and **7**, but attempts to isolate the isonitrile by preparative TLC on silica failed. Although the isonitrile **10** is stable to this type of chromatography, apparently **7** cyclizes on the preparative plate during chromatographic elution to provide **2**. It was suggested that the formation of **2** arises from a base-induced cyclization of the isonitrile.[9] However, the putative reaction sequence involves a phosphorylimide,[10] and this intermediate should behave in a manner analogous to that depicted in eq. 2. These results indicate that **2** can be derived either directly from an activated imine such as **5**, or can be formed by a more circuitous route through **7**. As we were unable to obtain pure **7**, assessing the reactivity of the isonitrile under the conditions of basic PTC was not possible.

The relative reactivity of $:CCl_2$ most likely is such that the carbene cannot sufficiently discriminate between the nitrogen of the primary amino moiety and the pyridyl ring nitrogen. Consequently, path *b* of Scheme I represents an important competing reaction sequence that leads to the production of unwanted products and reduced yields of **2**. This sequence is similar to the Fujiwara reaction, in which $CHCl_3$ reacts with pyridine in a solution of alkaline hydroxide.[11] The major products of the Fujiwara reaction are aldehydic imines and amidines derived from cleavage of the N-alkylated pyridine ring.[12] This reaction is performed under conditions consistent with the production of $:CCl_2$ and is inhibited with common carbene traps such as methanol.[13] Although the Fujiwara reaction is generally executed in single-phase media, other reactions have reportedly been performed under conditions of basic PTC with $CHCl_3$ and substituted pyridines that invoke mechanisms involving the reaction of $:CCl_2$ at the pyridyl ring nitrogen.[14] Moreover, various other carbenes (e.g., $:C(CN)_2$ and $:C(CO_2Et)_2$) are known to form stable ylides with pyridine and azanaphthalenes,[6,15] and recently it has been reported that

ylide intermediates are formed by the reaction of pyridine with phenylchlorocarbene.[16] In the case of 2-AMP, an analogous reaction is proposed in which the pyridyl ring nitrogen competes with the aminomethyl group for $:CCl_2$ to generate a $^{-}CCl_2$-pyridinium species (**8**). Assuming that the initial ylide survives to be protonated, such electron-deficient N-alkylated and N-acylated rings are extremely susceptible to reactions with nucleophiles at the *ortho* and *para* ring positions.[17,18] The carbene-promoted activation of the pyridyl ring undoubtedly leads to attack by ambient nucleophiles and the formation of numerous by-products and tars.

The reaction of chloroform under basic PTC with the 2-aminomethylpyridyl moiety appears to be general and can be applied to other systems. As shown in Table 1, the aminomethyl derivatives of both quinoline and isoquinoline can be converted into their corresponding imidazo analogs. Unfortunately, the yields of all the annulated products were in the 25% range, despite nearly complete consumption of the starting amines. Nevertheless, the reaction mixtures of the azanaphthalenes provided relatively simple gas chromatograms that were analogous to the results obtained for **1**. 2-(Aminomethyl)-quinoline (**11**) was converted into the imidazoquinoline **12** in 24% yield, and the only other significant component (<2%) detected by GC was a compound whose GC and MS data corresponded to that of N-(2-quinoylmethyl)formamide (**13**). Treatment of **17** produced the imidazo[5,1-a]isoquinoline (**18**) in 32% yield along with a minor amount of the formamide **16**. The 3-(aminomethyl)-isoquinoline (**20**) did not provide any of the expected imidazo[1,5-b]isoquinoline (**21**). The reaction of the 4-methoxyquinoline derivative **14** with $CHCl_3$ under basic PTC gave, in addition to the expected imidazo compound **15** and formamide **16**, a substantial amount of 4-methoxy-2-quinaldamide (~8%).

The overall progress of the reactions of $CHCl_3$ with the aminomethyl compounds was most accurately monitored by GC. The formation of the imidazo compounds increased linearly with time; however, before the starting material was completely consumed, the rate of product formation changed abruptly, and the concentration of the imidazo compound began to decline rapidly. Consequently, the products were evaluated for their stability to the reaction medium. In the absence of $CHCl_3$, the purified imidazopyridyl compounds were unaffected by the basic phase-transfer reaction conditions. However, the addition of $CHCl_3$ to these control reactions resulted in a measurable time-dependent reduction in the concentration of lumophore. This loss was not initially obvious when the reactions were monitored by TLC; however, analysis of the reaction mixtures by analytical GC clearly

indicated product consumption in the presence of $CHCl_3$. Exhaustion of the imidazopyridines did not result in the commensurate production of any identifiable compounds, but rather led to a menagerie of very minor products inseparable by TLC. The GC traces of these reactions were typified by a reduction in the intensity of the imidazo peak, and no additional compounds were present. The relative rates for consumption of the imidazo compounds in the presence of $CHCl_3$ under basic PTC conditions were evaluated, and the compounds' half-lives calculated: **2** (181 min) > **18** (131 min) > **12** (83 min) > **15** (72 min) (0.02M TAB, 1M $CHCl_3$, 1 mL DME, 1 mL 40% NaOH, 50°C). GC flame factors for the reaction products were also determined, and we found that the low isolated yields are an accurate measure of product formation and are not a result of the purification sequence.

Jones and Rees have described some reactions of $:CCl_2$ with pyrroles[19] and imidazoles[20] and have shown insertion of the carbene into the double bond of $-C_b=C_a-NH-$ is the primary reaction that leads to isolable products. Subsequent rearrangement of the bicyclo[3.1.0]hexyl compound provides the corresponding b-chloroheterocycle. While similar reactions may be important to the $CHCl_3$-dependent decomposition of the imidazo products reported here, an evaluation of this chemistry was beyond the scope of the present work.

Acknowledgment. This work performed under the auspices of the U.S. Department of Energy by Lawrence Livermore National Laboratory under Contract W-7405-Eng-48. The author thanks the U.S. Department of Energy Hazardous Waste Remedial Actions Program for financial support and Drs. James Epler and Michael Angel for their encouragement of this work.

Table 1. Products from the PTC reaction of $CHCl_3$ with a-(aminomethyl)pyridyl derivatives over aqueous base.

Substrate	Principal Product	Major Byproduct
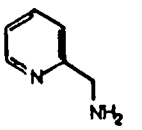 1	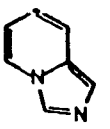 2 (26)[a]	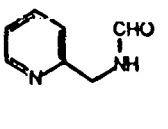 3 (<3)[b]
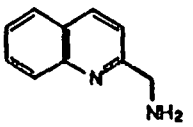 11	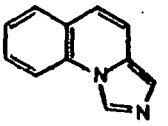 12 (24)[a]	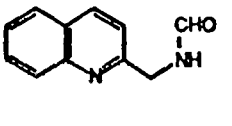 13 (<2)[b]
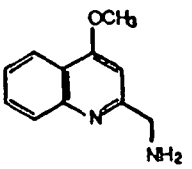 14	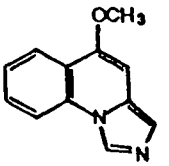 15 (18)[a]	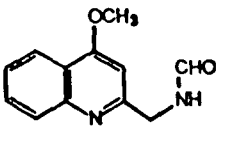 16 (9)[b]
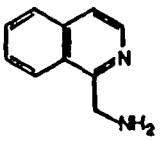 17	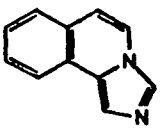 18 (32)[a]	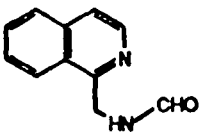 19 (<5)[b]
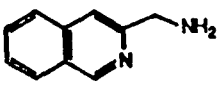 20	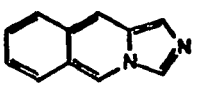 21 (0)	

(a) Isolated yield (b) GC yield.

Experimental Section

Melting points were obtained from samples in open capillary tubes and are uncorrected. Infrared (IR) spectra were obtained on an Mattson Polaris Fourier Transform Infrared spectrometer. Nuclear Magnetic Resonance (NMR) spectra were recorded on a Varian EM-390, a Bruker MSL-300, or a Nicolet 200-MHz spectrometer with tetramethylsilane as an internal standard. Low-resolution electron-impact mass spectra (EIMS) were recorded on a Hewlett-Packard Model 5987 mass spectrometer with direct sample insertion or by GC separation on a 0.32-mm x 30-m DB1 capillary column. High-resolution mass spectra (HRMS) were recorded at the Facility for Advanced Instrumentation at the University of California, Davis, on a VG ZAB-2H.

All thin-layer chromatography (TLC) was performed on Analtech (Newark, Delaware) precoated glass plates of silica gel GF. Analytical TLC to monitor reactions was accomplished with 0.25-mm silica gel plates briefly exposed to anhydrous ammonia. Chromatograms were visualized by illumination with a hand-held lamp emitting 254- or 366-nm light. Preparative TLC was performed on 20- x 20-cm plates coated to a thickness of either 0.50 or 1.0 mm of silica gel. Routine capillary gas chromatography was done on a Hewlett-Packard Model 5880 gas chromatograph using a 0.25-mm x 30-m DB1 column with an injector temperature of 250°C and an FID detector at 325°C. GC chromatograms were displayed and integrated by a Hewlett-Packard Level Two 5880A Series Terminal.

$CHCl_3$ was passed through neutral aluminum oxide (Brockmann activity I) to remove ethanol. 1,2-Dimethoxyethane was refluxed and distilled under nitrogen from calcium hydride. 2-(Aminomethyl)pyridine was obtained from Aldrich Chemical Co. and distilled at reduced pressure before use. The quinoline and isoquinoline aminomethyl dihydrochlorides were synthesized and their preparations will be reported elsewhere.

Imidazo[1,5-a]pyridine (2). To a mixture of 2-aminomethylpyridine (2.0 mL, 19.4 mmole) and tetrapropylammonium bromide (52 mg, 1.94 mmole) in 1,2-dimethoxyethane (20 mL) was added 20 mL of a 40% w/v solution of aqueous NaOH. As the two-phase solution was stirred rapidly at 55°C, $CHCl_3$ (2.0 mL, 25 mmole) was added in one portion. The reaction mixture was stirred under N_2 at 55°C and monitored periodically by TLC and GC. After 22 h, the rate of product formation had decreased, so 1.0 mL of $CHCl_3$ was added. After 28 h, GC indicated product formation had ceased. The dark-brown organic phase was collected, diluted with dichloromethane (50 mL), and washed with saturated aqueous KCl (2 x 30 mL). The aqueous phases were back-extracted with 3 x 30 mL of dichloromethane. The organic fractions were

combined, dried over anhydrous Na_2SO_4, filtered, and the solvents removed with a rotary evaporator. The thick, brown residue was chromatographed on a 2.5- x 30-cm column of silica gel (70-230 mesh) eluted with 5% acetonitrile in ethyl acetate. After an initial 100 mL of eluant, the product was collected in the following 250-mL volume. The solvent was removed under reduced pressure, leaving a brown residue that crystallized upon cooling. This material was condensed onto a cold finger (80°C, 1-2-mm Hg), giving 592 mg (26% yield) of white solid.

mp 53-54°C (lit.[3] 54-55°C);
IR (KBr, cm^{-1}) 3085, 1633, 1443, 1437, 1329, 1245, 1116, 996, 91, 795, 739, 657;
^1H NMR (90 MHz, DMSO-d_6) d 6.44-6.81 (m, 2H), 7.41-7.54 (m, 2H), 8.13-8.20 (d, 1H), 8.29 (s, 1H);.
EIMS *m/z* (relative intensity) 118 (100), 91 (24), 78 (18), 64 (42);
HRMS for $C_7H_6N_2$: calcd. 118.0531, found 118.0519.

Imidazo[1,5-a]quinoline (12). To a mixture of 2-aminomethylquinoline dihydrochloride (520 mg, 2.25 mmole) and tetrapropylammonium bromide (53 mg, 0.2 mmole) in 1,2-dimethoxyethane (10 mL) was added 10 mL of a 40% w/v solution of aqueous NaOH. The mixture was rapidly stirred, and when the solids had dissolved, the two-phase solution was heated to 50°C, and $CHCl_3$ (800 µL, 10 mmole) was added in one portion. The reaction mixture was stirred under N_2 at 50°C and monitored periodically by TLC (silica gel, 5% CH_3CN in EtOAc) and GC. After 16 h, the organic phase was collected, diluted with dichloromethane (30 mL), and washed with saturated aqueous KCl (2 x 30 mL). The organic fraction was dried over anhydrous Na_2SO_4, filtered, and the solvents removed with a rotary evaporator. The residue was chromatographed on two preparative thin-layer silica gel plates eluted with 7% acetonitrile in ethyl acetate. The major fluorescent fraction (R_f 0.4) was washed from the silica with 5% MeOH in CH_2Cl_2, the solvent removed, and the residue condensed onto a cold finger (90-95°C, 0.3-mm Hg), giving 92 mg (24% yield) of white solid.

mp 75-76°C (lit.[21] 73-75°C);
^1H NMR (200 MHz, acetone-d_6) d 7.13-7.18 (d, 1H), 7.42-7.51 (m, 3H), 7.58-7.68
(m, 1H), 7.77-7.83 (dd, 1H), 8.27-8.33 (dm, 1H), 8.91 (s, 1H);
IR (KBr, cm^{-1}) 3100, 1610, 1485, 1454, 1405, 1332, 1263, 1219, 1118, 926, 810, 758, 655;
EIMS *m/z* (relative intensity) 168 (100), 140 (30), 128 (21);
HRMS for $C_{11}H_8N_2$: calcd. 168.0687, found 168.0690.

Imidazo[5,1-a]isoquinoline (18). To a suspension of 1-aminomethylisoquinoline dihydrochloride (231 mg, 0.1 mmole) and tetrapropylammonium bromide (27 mg, 0.1 mmole) in freshly distilled 1,2-dimethoxyethane (5 mL) was added 5 mL of a 40% w/v solution of aqueous NaOH. $CHCl_3$ (400 µL, 10 mmole) was added in one portion, and the reaction was performed as for **12**. After 3.25 h, the concentration of product had reached its maximum value and the reaction mixture was worked up as for **12**. The residue was chromatographed on two preparative thin-layer silica gel plates eluted with 5% MeOH in CH_2Cl_2. The major fluorescent fraction (R_f 0.4) was collected, the solvent removed, and the residue sublimed onto a cold finger (95°C, 0.3-mm Hg), giving a white solid that was recrystallized from heptane (54 mg, 32% yield).

mp 115-116°C (lit.[21-23] 116-117°C);
IR (KBr, cm^{-1}) 3122, 3072, 1489, 1459, 1445, 1369, 1239, 1114, 912, 821, 793, 762, 656;
^1H NMR (200 MHz, acetone-d_6) d 6.92-6.96 (d, 1H), 7.41-7.60 (m, 12 lines, 2H), 7.68-7.73 (dm, 1H), 7.86 (s, 1H), 8.11-8.17 (dm, 2H), 8.25 (s, 1H);
EIMS *m/z* (relative intensity) 168 (100), 140 (33), 128 (8);
HRMS for $C_{11}H_8N_2$: calcd. 168.0687, found 168.0691.

5-Methoxyimidazo[1,5-a]quinoline (15). To a suspension of 2-aminomethyl-4-methoxyquinoline dihydrochloride (520 mg, 2.0 mmole) and tetrapropylammonium bromide (53 mg, 0.2 mmole) in freshly distilled 1,2-dimethoxyethane (10 mL) was added 10 mL of a 40% w/v solution of aqueous NaOH. $CHCl_3$ (800 µL, 20 mmole) was added in one portion and the reaction was performed as for **12**. After 8.0 h, the concentration of product had reached its maximum value, and the reaction mixture was worked up as for **12**. The residue was chromatographed on two preparative thin-layer silica gel plates eluted with a solution of 5% methanol in dichloromethane. The major fluorescent fraction (R_f 0.5) was collected, the solvent removed, and the brown residue sublimed onto a cold finger at reduced pressure (150°C, 0.3-mm Hg), giving 70 mg (18% yield) of white solid.

mp 131.5-132.5°C;
^1H NMR (300 MHz, $CDCl_3$) d 4.01 (s, 3H), 6.80 (s, 1H), 7.18 (s, 1H), 7.44-7.54 (m, 1H), 7.62-7.72 (m, 1H), 8.08-8.08 (dd, 1H), 8.24-8.30 (dm, 1H), 8.73 (s, 1H);
^{13}C NMR (75 MHz, $CDCl_3$) d 149.43, 131.17, 129.07, 128.71, 126.52, 124.91, 123.71, 120.11, 119.75, 114.17, 91.03, 55.29;
IR (KBr, cm^{-1}) 3098, 2967, 1631, 1565, 1486, 1460, 1400, 1359, 1277, 1211, 1139, 1103, 926, 820, 761, 652;
EIMS *m/z* (%) 198 (100), 183 (43), 155 (68);
HRMS for $C_{12}H_{10}N_2O$: calcd. 198.0793, found 198.0766.

Anal. calcd for $C_{12}H_{10}N_2O$: C, 72.71; H, 5.09; N, 14.13. Found: C, 72.77; H, 5.27; N, 13.81.

APPENDIX REFERENCES

1. (a) Angel, S. M.; "Optrodes: Chemically selective fiber-optic sensors," *Spectroscopy* **1987**, *2*, 38; (b) Seitz, W. R.; "Chemical sensors based on fiber optics," *Anal. Chem.* **1984**, *56*, 16A; (c) Peterson, J. I.; Vurek, G. G.; "Fiber optic sensors for biomedical applications," *Science* **1984**, *224*, 123.

2. Lerner, D. A.; Horowitz, P. M.; Evleth, E. M.; "Comparative photophysics of indolizine and related heterocycles," *J. Phys. Chem.* **1977**, *81*, 12.

3. Bower, J. D.; Ramage, G. R.; "Heterocyclic systems related to pyrrocoline. Part I. 2:3a-diazaindene," *J. Chem. Soc.* **1955**, 2834.

4. (a) Fodor, G.; Nagubandi, S.; "Correlation of the von Braun, Ritter, Bischler-Napieralski, Beckmann and Schmidt reactions via nitrilium salt intermediates," *Tetrahedron* **1980**, *36*, 1279. (b) Nagubandi, S.; Fodor, G.; "The Mechanism of the Bischler-Napieralski Reaction," *J. Heterocylic Chem.* **1980**, *17*, 1457.

5. Pierce, A.; Joullié, M. M.; " Observations on the formation of piperidine hydrochloride from chloroform and piperidine," *J. Org. Chem.* **1962**, *27*, 2220.

6. (a) Kirmse, W.; *Carbene Chemistry*, 2nd ed.; Academic Press: New York, 1971. (b) Sasson, Y.; Yonovich, M.; "The effect of phase transfer catalysts on the Reimer-Tiemann reaction," *Tetrahedron Lett.* **1979**, 3753. (c) Julia, S.; Ginebreda, A.; "A new method for the generation of dichlorocarbene using solid-liquid phase-transfer catalysis," *Synthesis* **1977**, 682. (d) Dehmlow, E. V.; "Advances in phase-transfer catalysis," *Angew. Chem., Int. Ed. Engl.* **1977**, *16*, 493.

7. (a) *Isonitrile Chemistry*, Ugi, I., Ed.; Academic Press: New York, 1971; Chapter 2. (b) Weber, W. P.; Gokel, G. W.; "An improved procedure for the Hofmann carbylamine synthesis of isonitriles," *Tetrahedron Lett.* **1972**, 1637.

8. (a) Smith, P. A. S.; Kalenda, N. W.; "Investigation of some dialkylamino isocyanides," *J. Org. Chem.* **1958**, *23*, 1599. (b) Halleux, A.; "α-Addition of dichlorocarbene to cyclohexyl isonitrile," *Angew. Chem. Int. Ed. Engl.* **1964**, *3*, 752. (c) Dehmlow, E. V.; Lissel, M.; "Nebenreaktionen der Dihalogencarbenerzeugung aus Haloform/Natronlauge/ Katalysator," *Chem. Ber.* **1978**, *111*, 3873.

9. Schöllkopf, U.; Eilers, E.; Hantke, K.; "N-[1-(3- und 4-Pyridyl)-1-alkenyl]formamide aus α-metallierten 3- bzw. 4-pyridylmethylisocyaniden und carbonylverbindungen; 3- und 4-acylpyridine, 1-(3-pyridyl)-1-alkylisocyanide," *Liebigs Ann. Chem.* **1976**, 969.

10. (a) Appel, R.; Kleinstrück, R.; Ziehn, K.-D.; "New preparation of isocyanides," *Angew. Chem., Int. Ed. Engl.* **1971**, *10*, 132. (b) Appel, R.; Warning, K.; Ziehn, K.-D.; "Über zwei neue verhahren zur darstellung von Imidhalogeniden," *Chem. Ber.* **1973**, *106*, 3450.

11. Uno, T.; Okumura, K.; Kuroda, Y.; "Mechanism of the Fujiwara reaction: structural investigation of reaction products from benzotrichloride," *J. Org. Chem.* **1981**, *46*, 3175.

12. Uno, T.; Okumura, K.; Kuroda, Y.; "The Fujiwara reaction: isolation and structural investigation of the reaction product from chloroform," *Chem. Pharm. Bull.* **1982**, *30*, 1876.

13. Langry, K. C. unpublished results.

14. (a) Berg-Nielsen, K.; "Synthesis of cyclopropyl-substituted heterocyclic compounds," *Acta Chemica Scand. B* **1977**, *31*, 224. (b) Arnoldi, A.; Galli, R.; Zagni, A.; "A novel reaction of dichlorocarbene with 2-chlorosubstituted nitrogen heteroaromatic bases under phase transfer conditions," *Heterocycles* **1979**, *12*, 1335.

15. Pomerantz, M.; Rooney, P.; "Relative rates of the reaction of (ethoxycarbonyl)carbene with several aromatic and heteroaromatic compounds. Selectivity and mechanism," *J. Org. Chem.* **1988**, *53*, 4374.

16. Jackson, J. E.; Soundararajan, N.; Platz, M. S.; Liu, M. T. H.; "Pyridine ylide formation by capture of phenylchlorocarbene and tert-butylchlorocarbene. Reaction rates of an alkylchlorocarbene by laser flash photolysis," *J. Amer. Chem. Soc.* **1988**, *110*, 5595.

17. (a) Rodig, O. R. "Quaternary Pyridinium Compounds," in *Pyridine and Its Derivatives, Supplement Part 1*, Abramovitch, R. A., Ed., John Wiley & Sons, New York, 1974. Chapter III. (b) Duchardt, K. H.; Kröhnke, F.; "(Trihalogenmethyl)-dihydropyridine," *Chem. Ber.* **1977**, *110*, 2669. (c) Lyle, R. E.; Gauthier, G. J.; "Reactions of nucleophiles with pyridinium ions. Cyanide ion reactions with some pyridinium ions." *Tetrahedron Lett.* **1965**, 4615. (d) Molyneux, R. J.; Wong, R. Y.; "Formation of enamine Schiff bases by ring cleavage of pyridine," *Tetrahedron* **1977**, 1931.

18. King, Jr., J. A.; Donahue, P. E.; Smith, J. E.; "Reaction of pyridine with phosgene: A structural reevaluation," *J. Org. Chem.* **1988**, *53*, 6145.

19. Jones, R. L.; Rees, C. W.; "Mechanism of heterocyclic ring expansions. Part III. Reaction of pyrroles with dichlorocarbene," *J. Chem. Soc. (C)* **1969**, 2249.

20. Jones, R. L.; Rees, C.; "Mechanism of heterocyclic ring expansions. Part IV. Reaction of an imidazole, pyrrole and 1,2,4-triazole with dichlorocarbene," W. *J. Chem. Soc. (C)* **1969**, 2251.

21. van Nispen, S. P. J. M.; Mensink, C.; van Leusen, A. M.; "Use of dilithio-tosylmethyl isocyanide in the synthesis of oxazoles and imidazoles," *Tetrahedron Lett.* **1980**, *21*, 3723.

22. Reimlinger, H.; Vandewalle, J. J. M.; Lingier, W. R. F.; de Ruiter, E.; "Kondensierte isochinoline, XI. Imidazo-[5,1-a]isochinoline," *Chem. Ber.* **1975**, *108*, 3771.

23. Zimmer, H.; Glasgow, D. G.; McClanahan, M.; Novinson, T.; "Imidazo[5,1-a]isochinoline," *Tetrahedron Lett.* **1968**, 2805.

INTERNAL DISTRIBUTION

1. R. E. Adams
2. B. A. Berven
3. R. J. Borkowski
4. D. W. Burton
5. T. R. Butz
6. R. B. Craig
7. B. M. Eisenhower
8. J. E. Emmons
9. J. L. Epler
10. L. D. Eyman
11. C. S. Fore
12. P. J. Franco
13. R. B. Gammage
14. R. K. Genung
15. J. M. Hoegler
16. G. R. Jasny
17. L. W. Long
18. J. F. McBrayer
19. C. P. McGinnis
20. L. J. Mezga
21. J. C. Parker
22. J. L. Petty
23. J. G. Rogers
24. N. E. Rothermich
25. J. S. Suffern
26. W. W. Thompson

27-76. HAZWRAP Library

77. ORNL Patent Office
78. Central Research Library
79. Document Reference Library
80. Laboratory Records Dept.
81. Laboratory Records, ORNL-RC

EXTERNAL DISTRIBUTION

DEPARTMENT OF ENERGY

82. S. Bolling, U.S. Department of Energy, Nevada Operations, P.O. Box 98515, Las Vegas, Nv 89193

83. R. T. A. Bredderman, U.S. Department of Energy, San Francisco Operations Office, Wells Fargo Bank Building, 1333 Broadway, Oakland, CA 94612

84. R. F. Brich, U.S. Department of Energy, Nevada Operations, P.O. Box 98518, MS 505, Las Vegas, Nevada 89193

85. D. S. Browning, Chemical Engineer, Process and Weapons Division, U.S. Department of Energy, Savannah River Operations Office, P.O. Box A, Aiken, SC 29802

86. R. L. Chandler, Director, Process and Weapons Division, U.S. Department of Energy, SavannahRiver Operations Office, P.O. Box A, Aiken, SC 29802

87. T. C. Chee, Office of Defense Waste and Transportation Management, U.S. Department of Energy, EP-123 (GTN), Washington, DC 20545

88. B. W. Church, U.S. Department of Energy, Nevada Operations Office, P.O. Box 98518, MS 505, Las Vegas, NV 89193

89. L. W. Clark, U.S. Department of Energy, Oak Ridge Operations Office, P.O. Box 2001, Oak Ridge, TN 37831

90. Fil Fong, U.S. Department of Energy, San Francisco Operations Office, Wells Fargo Bank Building, 1333 Broadway, Oakland, CA 94612

91. C. H. George, U.S. Department of Energy (GTN), Washington, DC 20545

92. J. D. Goodenough, U.S. Department of Energy, Richland Operations Office, P.O. Box 550, Richaland, WA 99352

93. J. C. Haugen, U.S. Department of Energy, Chicago Operations, 9700 S. Cass Avenue, Argonne, IL 60439

94. P. T. Hoopes, U.S. Department of Energy, Kansas City Area Office, 2000 E. 95th Street, Kansas City, MO 64131-3095

95. M. R. Jugan, U.S. Department of Energy, Savannah River Operations Office, P.O. Box 2001, Oak Ridge, TN 37831

96. S. King, U.S. Department of Energy, Savannah River Operations Office, P.O. Box A, Aiken, SC 29803

97. D. Krenz, U.S. Department of Energy, Albuquerque Operations Office, P.O. Box 5400, Albuquerque, NM 87115

98. J. C. Lehr, U.S. Department of Energy, Hazardous Waste and Remedial Actions Division, Office of Defense Waste and Transportation Management, DP-124 (GTN), Washington, DC 20545

99. D. M. Lund, U.S. Department of Energy, Albuquerque Operations Office, P.O. Box 5400, Albuquerque, NM 87107,

100. G. C. Marshall, U.S. Department of Energy, Argonne Area Office, 9700 S. Cass Avenue, Argonne, IL 60439

101. G. Runkle, U.S. Department of Energy, Albuquerque Operations Office, P.O. Box 5400, Albuquerque, NM 87185

102. D. Sanow, U.S. Department of Energy, Idaho Operations Office, 785 DOE Place, Idaho Falls, ID 83402

103. W. B. Schulze, U.S. Department of Energy, Richland Operations, Federal Building/Room 629, P.O. Box 550, Richland, WA 99352

104. M. W. Shupe, U.S. Department of Energy, Idaho Operations Office, 550 Second Street, Idaho Falls, ID 83401

105. C. Soden, U.S. Department of Energy, Albuquerque Operations Office, P.O. Box 5400, Albuquerque, NM 87185

106. J. E. Solecki, U.S. Department of Energy, Idaho Operations Office, 550 Second Street, Idaho Falls, ID 83401

107. D. E. Stamer, U.S. Department of Energy, Chicago Operations Office, 9800 S. Cass Avenue, Argonne, IL 60439

108. R. K. Stewart, U.S. Department of Energy, Richland Operations Office, P.O. Box 550, Richland, WA 99352

109. Hunter Weiler, U.S. Department of Energy, 785 DOE Place, Idaho Falls, ID 83402

110. S. R. Wright, Director, Environmental Division, U.S. Department of Energy, Savannah River Operations Office, P.O. Box A, Aiken, SC 29802

111. Office of Assistant Manager for Energy Research and Development, U.S. Department of Energy, Oak Ridge Operations Office, P.O. Box E, Oak Ridge, TN 37831

112.-113. Office of Scientific and Technical Information, U.S. Department of Energy, P.O. Box 62, Oak Ridge, TN 37831

DOE CONTRACTORS

114. R. E. Anderson, Martin Marietta Energy Systems, Inc., P.O. Box 628, Piketon, OH 45661

115. C. Ariss, EG&G Idaho, Inc., Idaho National Engineering Laboratory, P.O. Box 1625, Idaho Falls, ID 83415-2212

116. J. G. Avery, Los Alamos National Laboratory, MS J576, Los Alamos, NM 87545

117. K. Balo, Los Alamos National Laboratory, MS J592, Los Alamos, NM 87545

118. K. Barclay, MSE, Idaho National Engineering Laboratory, P.O. Box 4078, Butte, MT 59702

119. R. A. Bari, Associated Universities, Inc., Brookhaven National Laboratory, Building 130, Upton, NY 11973

120. J. M. Beller, EG&G Idaho, Inc., Idaho National Engineering Laboratory, P.O. Box 1625, MS 2208, Idaho Falls, ID 83415

121. J. J. Blakeslee, Rockwell International, Rocky Flats Plant, P.O. Box 464, Golden, CO 80402-0464

122. R. K. Blauvelt, EG&G Corporation, Mound Facility, P.O. Box 32, Miamisburg, OH 45342

123. L. C. Borduin, Los Alamos National Laboratory, MS E517, Los Alamos, NM 87545

124. S. S Borys, Argonne National Laboratroy, Building 208, 9700 Cass Avenue, Argonne, IL 60439

125. J. W. Cammann, Westinghouse Hanford Company, 450 Hill Street, Richland, WA 99352

126. B. Chantrill, EG&G Idaho, P.O. Box 1625, MS 3528, Idaho Falls, ID 83415

127. H. O. Charnock, 2750E/D126/200W, Westinghouse Hanford Company, P.O. Box 1970, Richland, WA 99352

128. C. L. Cheever, Argonne National Laboratory, 9700 South Cass Avenue, Argonne, IL 60439

129. P. Colombo, Associated Universities, Inc., Brookhaven National Laboratories, Building 703, Upton, NY 11973

130. J. R. Cook, Savannah River Laboratory, Building 773-43A, Room 209, Aiken, SC 29808

131. J. C. Corey, Research Manager, Environmental Sciences Division, Savannah River Laboratory, Aiken, SC 29808

132. R. M. Cranwell, Division 6416, Sandia National Laboratories, Albuquerque, NM 87185-5800

133. R. L. Dodge, Radioactive Waste Management, MS 738, Reynolds Electrical & Engineering Co., P.O. Box 98521, Las Vegas, NV 89193-8521

134. L. L. Ebeling, Reynolds Electrical & Engineering Co., Nevada Test Site, P.O. Box 564, Mercury, NV 89023

135. D. F. Emer, Radioactive Waste Management, MS 738, Reynolds Electrical & Engineering Co., P.O. Box 98521, Las Vegas, NV 89193-8521

136. L. Emma, Brookhaven National Laboratory, Upton, Long Island, NY 11973

137. S. A. Felecetti, Division 3314, Sandia National Laboratories, Albuquerque, NM 87185-5800

138. A. C. Ficklin, Rockwell Internation, Energy Systems Group, Rocky Flats Plant, P.O. Box 464, Golden, CO 80401

139. E. Franz, Brookhaven National Laboratory, Upton, Long Island, NY 11973

140. W. Freeman, Fermi National Accelerator Laboratory, P.O. Box 500, Batavia, IL 60510

141. K. Gentry, Allied-Signal, Inc., Bendix Kansas City Division, P.O. Box 419159, D/186, BD59, Kansas City, MO 64141-6159

142. T. E. Hakonson, Los Alamos National Laboratory, MS K495, Los Alamos, NM 87545

143. W. R. Hansen, Los Alamos National Laboratory, MS F643, Los Alamos, NM 87545

144. J. N. Hartely, Sigma 5/3000 Area, Battelle Pacific Northwest Laboratories, P.O. Box 999, Richland, Washington 99352

145. O. L. Haworth, Reynolds Electrical & Engineering Co., Nevada Test Site, 6404 Peppermill Drive, Las Vegas, NV 89102

146. W. F. Heine, Westinghouse Hanford Operations, P.O. Box 800, Richland, WA 99352

147. J. Helt, Argonne National Laboratory, 9700 South Cass Avenue, Argonne, IL 60439-4837

148. B. D, Helton, Building 703-H, Savannah River Plant, P.O. Box A, Aiken, SC 29801

149. D. A. Hoyte, University of California, Lawrence Livermore National Laboratory, P.O. Box 808, L-620, Livermore, CA 94550

150. S. Johnston, Sandia National Laboratories, Division 8356, P.O. Box. 808, Albuquerque, NM 87185-8356

151. K. Jordan, Westinghouse Hanford Company, P.O. Box 550, Richland, WA 99352

152 E. W. Kendall, Radioactive Waste Management, MS 738, Reynolds Electrical & Engineering Co., P.O. Box 98521, Las Vegas, NV 89193-8521

153. K. M. King, Radioactive Waste Management, MS 738, Reynolds Electrical & Engineering Co., P.O. Box 98521, Las Vegas, NV 89193-8521

154. S. Koegler, Pacific Northwest Laboratories, P.O. Box 999, Richland, WA 99352

155. R. Koenig, Los Alamos National Laboratory, E518, Los Alamos, NM 87545

156. M. Larsen, EG&G Idaho, Inc., Idaho National Engineering Laboratory, P.O. Box 1625, Idaho Falls, ID 83415

157. C. D. Leigh, Division 6416, Sandia National Laboratories, Albuquerque, NM 87185-8500

158. B. Luth, Sandia National Laboratories, Geosciences Department 6230, Albuquerque, NM 87185

159. T. J. McLaughlin, Environmental & Risk Assessment Section, Radiological Sciences Department, Battelle Pacific Northwest Laboratories, P.O. Box 999, Richland, WA 99352

160. G. E. Millard, 3314, Sandia National Laboratories, Albuquerque, NM 87185

161. O. M. Morris, Jr., Superintendent, Waste Management Technology, Savannah River Laboratory, Aiken, SC 29808

162. K. M. Myles, Argonne National Laboratory, Building 205, 9700 South Cass Avenue, Argonne, IL 60439

163. N. R. Ortiz, Division 6410, Sandia National Laboratories, Albuquerque, NM 87185-8500

164. R. M. Ostmeyer, Division 6416, Sandia National Laboratories, Albuquerque, NM 87185-8500

165. J. M. Phelan, Division 3314, Sandia National Laboratories, Albuquerque, NM 87185-8500

166. R. R. Piscitella, EG&G Idaho, P.O. Box 1625, MS 3528, Idaho Falls, ID 83415

167. T. Poff, Westinghouse Corporation, Willey Road, P.O. Box 39158, Cincinnati, OH 45239

168. J. M. Ramirez, Allied-Signal, Inc., Bendix Kansas City Division, P.O. Box 419159, D/144, OB29, Kansas City, MO 64141-6159

169. T. L. Rasmussen, EG&G Idaho, P.O. Box 1625, Idaho Falls, ID 83415

170. K. H. Rea, Los Alamos National Laboratory, MS K490, Los Alamos, NM 87545

171. R. P. Rechard, Division 6416, Sandia National Laboratories, Albuquerque, NM 87185-5800

172. C. K. Rofer, Los Alamos National Laboratory, MS D462, Los Alamos, NM 87545

173. A. D. Rogers, EG&G Idaho, P.O. Box 1625, Idaho Falls, ID 83415

174. N. F. Sather, Argonne National Laboratory, Building 362, 9700 S. Cass Avenue, Argonne, IL 60439

175. W. C. Schutte, EG&G Idaho, Inc., Idaho National Engineering Laboratory, P.O. Box 1625, Idaho Falls, ID 83415

176. K. Siegfreidt, Sandia National Laboratories, Division 8311, Livermore, CA 94330

177. G. J. Smith, Division 3314, Sandia National Laboratories, Albuquerque, NM 87185-8500

178. E. Malone Steverson, EG&G Idaho, Inc., P.O. Box 1625, Idaho Falls, ID 83415-8101

179. T. L. Stewart, PSL/3000 Area, Battelle, Pacific Northwest Laboratories, P.O. Box 999, Richland, WA 99352

180. G. E. Streit, Los Alamos National Laboratory, MS F611, Los Alamos, NM 87545

181. H. F. Strum, Jr., Research Supervisor, Interim Waste Technology Division, Savannah River Laboratory, Aiken, SC 29808

182. D. F. Suciu, EG&G Idaho, Inc., Idaho National Engineering Laboratory, P.O. Box 1625, MS 2208, Idaho Falls, ID 83415

183. A. Tompson, University of California, Lawrence Livermore National Laboratory, Earth Sciences, L-206, P.O. Box 808, Livermore, CA 94550

184. R. L. Treat, Pacific Northwest Laboratories, P.O. Box 999, Richland, WA 99352

185. J. C. Umbarger, Los Alamos National Laboratory, MS K493, Los Alamos, NM 87545

186. P. J. Valenti, West Valley (Westinghouse), P.O. Box 141, West Vallely, NY 14171

187. J. L. Warren, Los Alamos National Laboratory, MS E516, Los Alamos, NM 87545

188. J. L. Williams, Paducah Gaseous Diffusion Plant, P.O. Box 1410, Paducah, KY 42001

189. G. T. Wright,.Research Manager, Interim Waste Technology Division, Savannah River Laboratory, Aiken, SC 29808

190. J. G. Yeager, Sandia National Laboratories, Organization 3314, Albuquerque, NM 87048

HAZWRAP TECHNOLOGY REVIEW GROUP

191. T. A. Burke, New Jersey Department of Health, Division of Occupational and Environmental Health, CN 360, Trenton, 08625

192. M. J. Carricato, Defense Department, 206 North Washington Street, Suite 100, Alexandria, VA 22314-2528

193. G. S Goldstein, Arthur D. Little, Inc., Acorn Park, Cambridge, MA 02140

194. P. E. LaMoreaux, Environmental Institute for Waste Management Studies, P.O. Box 2310, Tuscaloosa, AL 35043

195. F. Parker, Vanderbilt University, School of Environmental Engineering, P.O. Box 1596, Station B, Nashville, TN 37235

196. G. Paulson, The Center for Hazardous Waste Management, ITT Center, 10 West 35th Street, Chicago, IL 60616

197. S. Ragone, Office of Hazardous Waste Hydrology, 410 National Center, U.S. Geological Survey, Reston, VA 22092

198. B. S. Ruhl, Legal Environmental Assistance Foundation, 203 North Gadsden Street, Suite 7, Tallahassee, FL 32301

Technical Information Department • Lawrence Livermore National Laboratory
University of California • Livermore, California 94550